



**HAL**  
open science

## Marine karstic infillings: evidence of extreme base level changes and geodynamic consequences (Paleocene of Languedoc, south of France)

Eglantine Husson, Michel Seranne, Pierre-Jean Combes, Hubert Camus, Bernard Peybernes, M. J. Fondécave-Wallez, Mihaela Melinte-Dobrinescu

### ► To cite this version:

Eglantine Husson, Michel Seranne, Pierre-Jean Combes, Hubert Camus, Bernard Peybernes, et al.. Marine karstic infillings: evidence of extreme base level changes and geodynamic consequences (Paleocene of Languedoc, south of France). Bulletin de la Société Géologique de France, 2012, 183 (5), pp.425-441. 10.2113/gssgfbull.183.5.425 . hal-00767556

**HAL Id: hal-00767556**

**<https://hal.science/hal-00767556>**

Submitted on 7 Jun 2023

**HAL** is a multi-disciplinary open access archive for the deposit and dissemination of scientific research documents, whether they are published or not. The documents may come from teaching and research institutions in France or abroad, or from public or private research centers.

L'archive ouverte pluridisciplinaire **HAL**, est destinée au dépôt et à la diffusion de documents scientifiques de niveau recherche, publiés ou non, émanant des établissements d'enseignement et de recherche français ou étrangers, des laboratoires publics ou privés.

## Marine karstic infillings: evidence of extreme base level changes and geodynamic consequences (Paleocene of Languedoc, south of France)

EGLANTINE HUSSON<sup>1</sup>, MICHEL SÉRANNE<sup>1</sup>, PIERRE-JEAN COMBES<sup>1</sup>, HUBERT CAMUS<sup>2</sup>, BERNARD PEYBERNÈS<sup>1</sup>, MARIE-JOSÉ FONDECAVE-WALLEZ<sup>3</sup>, MIHAELA CARMEN MELINTE-DOBRINESCU<sup>4</sup>

*Keywords.* – Paleokarsts, Base level, Paleocene, Endoreic basin.

*Abstract.* – Late Jurassic platform carbonates of Languedoc (southern France) are deeply incised by Late Miocene canyons, allowing the observation of karst systems filled with sediments containing evidences of marine origin. Field and structural relationships as well as new biostratigraphic data (planktonic foraminifera and calcareous nannofossils) provide a Latest Cretaceous-Earliest Paleocene age for the major karstification and a Paleocene (Danian-Selandian) age for the sedimentary filling. The  $\geq 350$  m vertical extent of this karst system and its subsequent marine filling gives a minimum amplitude for the base-level variation responsible for the karstification and then the marine flooding events. The observations suggest that at least, two marine successive events occurred in the Late Danian then in Selandian time. The large amplitude of base level is not in agreement with eustatic sea-level change, and the rate of base-level change is too fast for tectonic uplift and subsidence within the tabular, poorly deformed studied area. We propose a model of a silled endoreic basin, which was dessiccated and karstified over hundreds of meters, when it was disconnected from the World Ocean, and later suddenly transgressed by the Paleocene sea and the karst flooded, when the bounding sill was submerged. Such a model is similar, although with significant differences, with the later Messinian-Zanclean event that affected the Mediterranean realm.

### Remplissages marins karstiques : évidence de variations extrêmes du niveau de base et conséquences géodynamiques (Paléocène du Languedoc, sud de la France)

*Mots-clés.* – Paléokarsts, Niveau de base, Paléocène, Bassin endoréique.

*Résumé.* – La plate-forme carbonatée d'âge jurassique supérieur du Languedoc (sud de la France) est profondément incisée au Miocène par des canyons, permettant ainsi d'observer un système karstique développé sur toute l'épaisseur du massif, contenant des sédiments internes d'origine marine. Les relations structurales de terrain ainsi que de nouvelles données biostratigraphiques, comme les foraminifères planctoniques et notamment des déterminations sur nannofossiles calcaires, révèlent un âge crétacé terminal à paléocène précoce pour la phase majeure de karstification et un âge paléocène (Danien-Sélandien) pour un remplissage des cavités. Le développement vertical de ce système karstique sur plus de 350 m et les remplissages sédimentaires marins qui ont suivi, contraignent une valeur minimum de l'amplitude de variation du niveau de base, responsable de la karstification, puis de l'envoieement marin. Nos observations indiquent l'existence d'au moins deux phases successives d'envoieement marin, au Danien supérieur puis au Sélandien. La grande amplitude de variation du niveau de base est excessive pour des variations eustatiques. De plus, la vitesse de variation semble trop élevée pour des surrections et des subsidences dans cette zone peu déformée et tabulaire. Nous proposons un modèle de bassin endoréique à seuil, soumis à assèchement et karstification sur plusieurs centaines de mètres d'épaisseur, lorsqu'il fut déconnecté de l'océan global, puis brutalement inondé par la mer et les karsts envoyés, lorsque le seuil fut immergé. Un tel modèle est similaire, bien que distinct sur plusieurs modalités, avec l'événement messino-zancléen qui a affecté plus tard le domaine méditerranéen.

## INTRODUCTION

Karstification by dissolution of carbonate rocks such as limestones or dolostones being mostly a destructive process, karsts are therefore hardly used as a direct geological recording tool. Indeed, karstic cavities may sometimes trap and preserve fossiliferous sediments, such as the phosphorite-filled karsts from SW France (Quercy) that yielded a very

diversified Oligocene vertebrate fauna [Legendre *et al.*, 1997] or the prehistoric human dwellings whose sedimentary-fill yield a comprehensive record of the Quaternary environments. Speleothems can often develop on the cavity walls due to the interplay of dissolution, percolation and precipitation of carbonates, mostly under the control of climate parameters. High-resolution analyses of oxygen isotopes in the concretions yield paleoclimatic proxies for the

1. Géosciences Montpellier, Université Montpellier 2, 34095 Montpellier cedex 05, France.

2. Cenote, 1 Chemin de Valdegour, 30900 Nîmes, France.

3. Géosciences Environnement Toulouse, Université Paul-Sabatier, 14 avenue Edouard-Belin, 31400, Toulouse, France

4. National Institute of Marine Geology and Geo-ecology (GEOECOMAR), 23-25 Rue Dimitrie Onciul, Bucharest, RO-024053 Roumanie

Corresponding author: M. Séranne. e-mail: michel.seranne@gm.univ-montp2.fr

Manuscript deposited on July 26, 2011; accepted on February 29, 2012.

Pleistocene [Plagnes *et al.*, 2002]. For older periods, early-middle Cretaceous paleokarst developments and bauxite infill have provided evidences for paleoenvironments and paleoclimates [Combes, 1990]. More recently, paleokarsts have been recognized as geological records [James and Choquette, 1988; Molina *et al.*, 2000; Bruxelles, 2001; Audra *et al.*, 2001; Baceta *et al.*, 2007; Calner *et al.*, 2010].

Karst development is controlled by the changes in base-level. For gravity karsts [Mangin, 1982], drops of base level can be quantified by the vertical extent of karst development. When the base level rises, the previously formed karstic network is flooded and marine sediments may be introduced and preserved from erosion in the cavities and lapiaz. Karst formation and its subsequent sedimentary filling can thus be used as a recording tool of the amplitude of base level changes. For example, foraminifera found in elevated caves in Bermuda allowed to determine a high-stand, 21 m higher than the present age, one during Marine Isotope Stage 11 [Van Hengstum *et al.*, 2009]. The processes responsible for base-level variation belong either to eustasy (sea level rise and fall) or to tectonic vertical movements (uplift and subsidence). An extreme case of sea-level drop occurred in relation with the Messinian desiccation of the Mediterranean sea, during the end of Miocene times, and led to the development of deep karsts within the surrounding margins [e.g. Audra *et al.*, 2004].

The Jurassic platform carbonates, presently exposed in Languedoc (southern France), have recorded a polyphase karstic history since their subaerial exposure [Peybernès and Combes, 1999; Charcosset *et al.*, 2000; Camus *et al.*, 2004]. However, the discovery of fossiliferous marine

Paleocene deposits trapped within paleokarsts throughout this part of southern France [Peybernès *et al.*, 2003; Combes *et al.*, 2007], suggests that a transgression occurred after the karstification. It also provides a precious constraint for chronological record and for the estimate of the amplitude of base-level variation.

The main objective of this contribution is to analyze the paleokarst features, including outcrops, microfacies of internal sediment, and micropaleontologic content (foraminifera and nannofossils) of successive infillings. The mapping of the vertical distribution of these paleokarsts, which depends on the amplitude of the base-level change, and of marine sediments assigned to Early-Middle Paleocene, suggests extreme amplitudes (> 350 m) of variations. Then we discuss the possible origin of base-level changes controlled either by sea-level and/or geodynamics. Finally, we find that the fast and extreme amplitude of base-level drop and rise points to the desiccation/drowning cycles of a silled endoreic basin, partly similar to the Messinian-Zanclean event in the Mediterranean realm. The use of such base-level markers allows to better constrain the geodynamic evolution of subaerially exposed areas, otherwise devoid of geological record.

## GEOLOGICAL SETTING AND LOCATION

The Mesozoic carbonate series in Languedoc were deposited from Lias to Earliest Cretaceous, on the northwestern margin of the Tethyan Ocean, controlled by N-E trending faults e.g. the Cévennes fault system [Baudrimont and Dubois, 1977; Lemoine *et al.*, 1986; Bonijoly *et al.*, 1996].

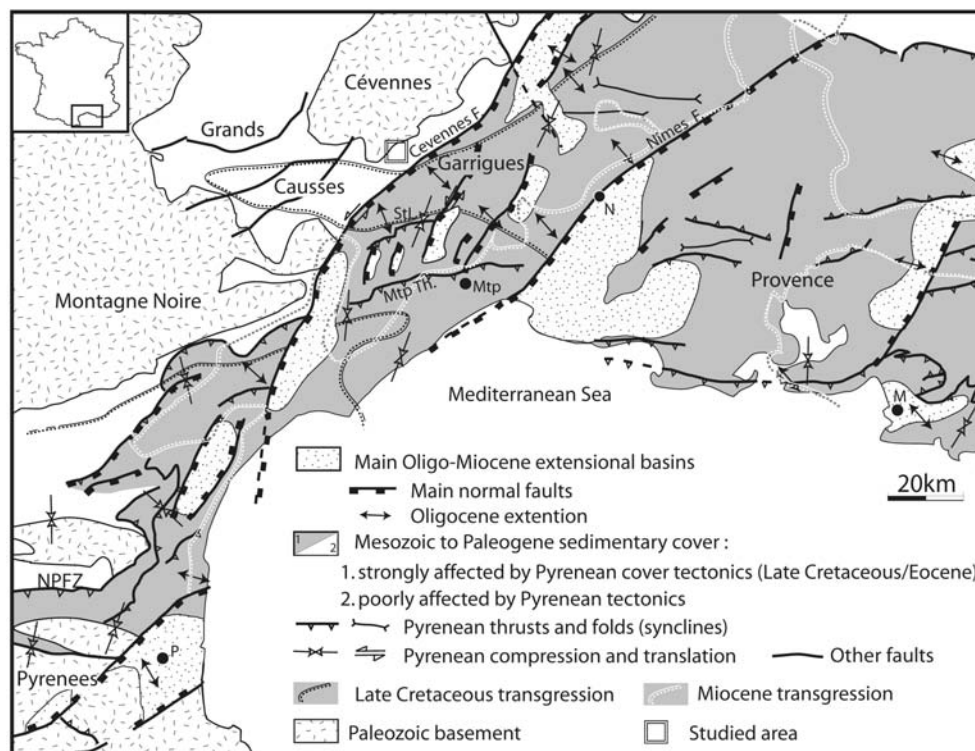


FIG. 1. – Location of the studied area (square) within a structural map of southern France [Benedicto, 1996, modified]. NPFZ: North Pyrenean fault zone, M: Marseille, Mtp: Montpellier, N: Nîmes, P: Perpignan, StL Th: Pic Saint Loup thrust, Mtp Th: Montpellier thrust.

FIG. 1. – Localisation de la zone d'étude (carré) dans le contexte structural du sud de la France [modifiée d'après Benedicto, 1996].

During Middle Cretaceous times, an inversion phase uplifted an E-W oriented shoal in southern France from Provence to Languedoc [“Isthme Durancien”, according to classic literature, see Baudrimont and Dubois, 1977]. Well documented in the neighboring basement rocks by apatite fission track analyses [Barbarand *et al.*, 2001], the associated denudation caused erosion and karstification of the Mesozoic carbonate platforms, leading to an important hiatus, increasing westward, and the formation of the bauxite-filled karsts in Languedoc [Combes, 1990]. The shallow marine sedimentation resumed in Turonian [Alabouvette *et al.*, 1984; Bruxelles *et al.*, 1999] (fig. 1) then became continental in Maastrichtian times, induced by the latest Cretaceous tectonics [Bruxelles, 2001]. Languedoc is classically described as a continental area since the end of Cretaceous, with deposition of fluvio-lacustrine “Rognacian” and “Vitrollian” facies [Freytet, 1970; Freytet and Plaziat, 1982], which took place during the progressive development of the E-W oriented Montpellier thrust. During the Pyrenean orogeny, Eocene in age, the N-E trending Cevennes fault was reactivated as a left-lateral ramp, which separates E-W folds and thrusts to the southeast, from flat-lying, poorly deformed surfaces to the northwest [Arthaud and Séguret, 1981; Arthaud and Laurent, 1995; Lacombe and Jolivet, 2005] (fig. 1). This event is dated by continental syn-tectonic deposits of Paleocene-Eocene age [Alabouvette *et al.*, 1984]. During the Oligocene, rifting of the Gulf of Lion [Séranne, 1999] occurred south of the studied area, and many regional faults, particularly the Cevennes fault, were reactivated as normal faults (fig. 1). From this time onwards, the drainage system flowed southwards, from the Cevennes basement high to the newly formed Gulf of Lion margin [Séranne *et al.*, 1995]. The last transgression event occurred during the Early Miocene (Burdigalian) in relation with the NW Mediterranean opening (fig. 1). Then a several hundred meters uplift affected the area during Late Miocene; this event resulted in the deep incision of the river network within the uplifted tabular Mesozoic carbonates [Séranne *et al.*, 2002]. During the Messinian event, the base level fall of 1500 m induced the incision of the major rivers in southern France (e.g. the Rhône canyon [Clauzon, 1982]), and the deepening of the karst systems in the carbonate plateaus, in order to adapt the drainage profile to the dessiccated endoreic basin [Audra *et al.*, 2004; Mocochain *et al.*, 2006].

The studied area, north of Montpellier (Ganges), is located just north of the Cevennes fault, which separates the tabular “Grands Causses”, Jurassic in age, and more to the SE the folded and faulted “Garrigues” area (see fig. 1 [Arthaud and Laurent, 1995; Arthaud and Séguret, 1981]). In this area, Late Jurassic carbonate rocks, locally dolomitized, dip 15-20° towards the SE (fig. 2). This region was chosen because: i) the calcareous formations displaying numerous paleokarstic features, are deeply incised by the Hérault and Rieutord rivers, which formed circa 400 m deep-canyons. So the Late Miocene incision of the streams allows the exceptional observation of the vertical distribution of the sediments which fill the numerous cavities of the karst systems; ii) this area, which is located north of the Cevennes fault, has been less affected by the Eocene “Pyrenean” tectonics; it allows to minimize the effects of the deformation in the measurement of base level change.

## STRUCTURAL FIELD RELATIONSHIPS

Exposed paleokarstic cavities display infillings that can be either parallel to the 15-20° dipping stratification of the Upper Jurassic host-rock, or horizontal. The former paleokarst filling predates the regional tilting whereas the latter occurred after deformation. This observation clearly supports polyphase karstic filling.

Some stratified karstic infillings are affected by meter-scale, north-verging, reverse faulting that induced formation of an E-W fold (fig. 3). These structures correspond to a N-S compression. Sets of meter-scale conjugated vertical strike-slip faults (N150 and N040) offset the Jurassic limestones. The slickensides provide the sense of displacement, which is consistent with a N-S oriented compression. These slickensides smear a reddish silty karstic infilling, suggesting a probable pre-tectonic karst. Finally, an outcrop displays remains of undeformed, horizontally stratified karstic infill, superimposed onto the walls of one of these strike-slip faults, corroded by a later stage of karstification (fig. 4). It is therefore a karst infilling that post-dates the activity of the fault.

On the base of structural relationships, three successive phases of karst infillings can be distinguished: i) infilling parallel to the bedding of the calcareous host-rocks, prior to the regional tilting; ii) horizontal infillings, postdating the regional tilting and predating the N-S compression which affected the area, in relation with the Late Cretaceous-Eocene Pyrenean orogeny; iii) undeformed infilling superimposed onto Pyrenean related structures.

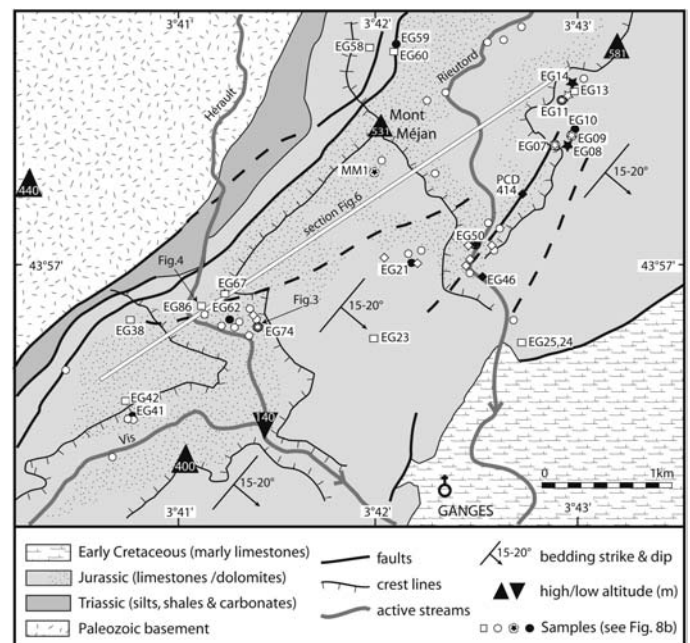


FIG. 2. – Detailed geologic and morphologic map of the studied area (location in fig. 1). Position of figures 2, 3 and 6, as well as analysed samples is given. Numbered samples have provided age constraint.

Fig. 2. – Carte géologique et morphologique détaillée de la zone d'étude (située fig. 1). Les positions des figures 2, 3, et 6 ainsi que celles des échantillons analysés sont indiquées, Les numéros montrent ceux qui sont datés.



FIG. 3. – Karstic cavity affected by a small-scale thrust. Internal sediments (dotted lines) are folded by a north-verging reverse fault related to the Pyrenean compression.

FIG. 3. – Cavit  karstique affect e par un chevauchement de petite  chelle. Les s diments internes (en pointill s) sont pliss s par une faille inverse de vergence nord induite par la compression pyr n enne.

The paleokarst infillings can thus record information within the karst, and their structural relationships with the host-rock allow to bracket their age, relative to tectonic events affecting the region, since the deposition of the Mesozoic carbonate platform.

## FACIES AND DATING OF THE KARSTIC INFILLINGS

Most observed infillings in the karstic cavities have been sampled.

### Dating methods

Most observed infillings in the karstic cavities have been sampled for sedimentologic facies analyses and biostratigraphic determinations. Numerous (80) thin-sections (45x30 mm) have been cut from indurated mudstones and siltstones internal sediments. Foraminifera and bioclasts were observed in section; investigation of washing residues from the rare occurrences of marly internal sediments were unsuccessful. Foraminifera are observed in light microscope at x120 magnification. Determination results from interpretation of different sections randomly cut across (axial and equatorial sections are rather rare). Recrystallisation, oxidation, dissolution and corrosion of foraminifera resulting from depositional, reworking and diagenetic processes are obstacles to determination. Overall, only 14 samples yielded foraminifera, belonging to 3 families of trochospiral planktic foraminifera corresponding to 8 genera and 10 different taxa.

Samples for the calcareous nannofossil analyses have been studied by light microscope, at x1600 magnification. No ultrasonic cleaning or centrifuge concentration was applied, in order to preserve the original biogenic composition of the rock-samples. The smear-slides were prepared

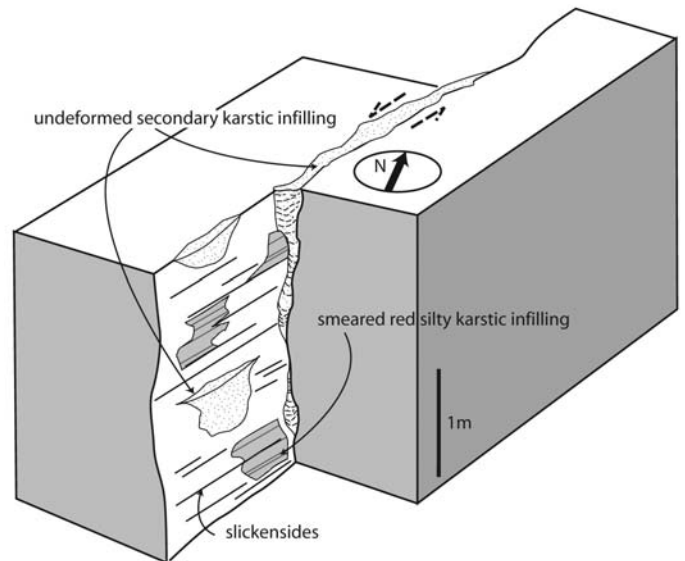


FIG. 4. – Structural relationships of two successive karstic infillings. A first generation of red silty infilling is observed smeared onto the strike-slip fault plane (pre-tectonic), while a second generation of undeformed silt and sandstone karstic infilling overprints the strike-slip fault (post-tectonic).

FIG. 4. – Relation structurale de deux remplissages karstiques successifs. Une premi re g n ration de remplissages silteux rouges est affect e par le jeu de la faille d crochante (pr -tectonique), alors qu'une seconde g n ration de remplissage karstique constitu e de sables et silts non d form e, se superpose   la faille d crochante (post-tectonique).

from the untreated sediment, following standard procedures, as follows: nannofossils were investigated in the fraction of 2-30  $\mu\text{m}$  separated by decantation method using 7% solution of  $\text{H}_2\text{O}_2$ . The heavy-fraction was allowed to settle for 5 minutes in a 55 mm water column and removed, while the fine-fraction was saved for slide preparation after 45 minutes. From the total encountered nannofloras, between 50-60% of taxa were difficult to be specifically assigned, due to their dissolution and/or overgrowth. Hence, the overall preservation of the calcareous nannoplankton could be considered moderate to poor.

Four types of infillings facies can be distinguished in the studied area.

### Facies A (stars in fig. 6 and 8)

All occurrences of pre-tilting karstic infillings display Facies A, but this facies may also be observed in the post-tilting karsts. It corresponds to a laminated wackestone, whose color varies from beige to different shades of pink, ocher or red, according to the composition of iron oxi-hydroxide content (fig. 5). The lamination results from alternating grain size (fine to very fine). The microfacies is a gray micritic to microsparitic carbonate mud including few grains of quartz (fig. 5). The layering visible at macroscopic scale results from the occurrence of fine beds of bioclasts. This low-energy facies results from settling of fine sediments. A karstic infill of Facies A has been found only in the upper parts of the incised canyons, above an altitude of 400 m (fig. 6).

The samples characterizing facies A are rich in marine fauna and diversified bioclasts including: echinoderms,

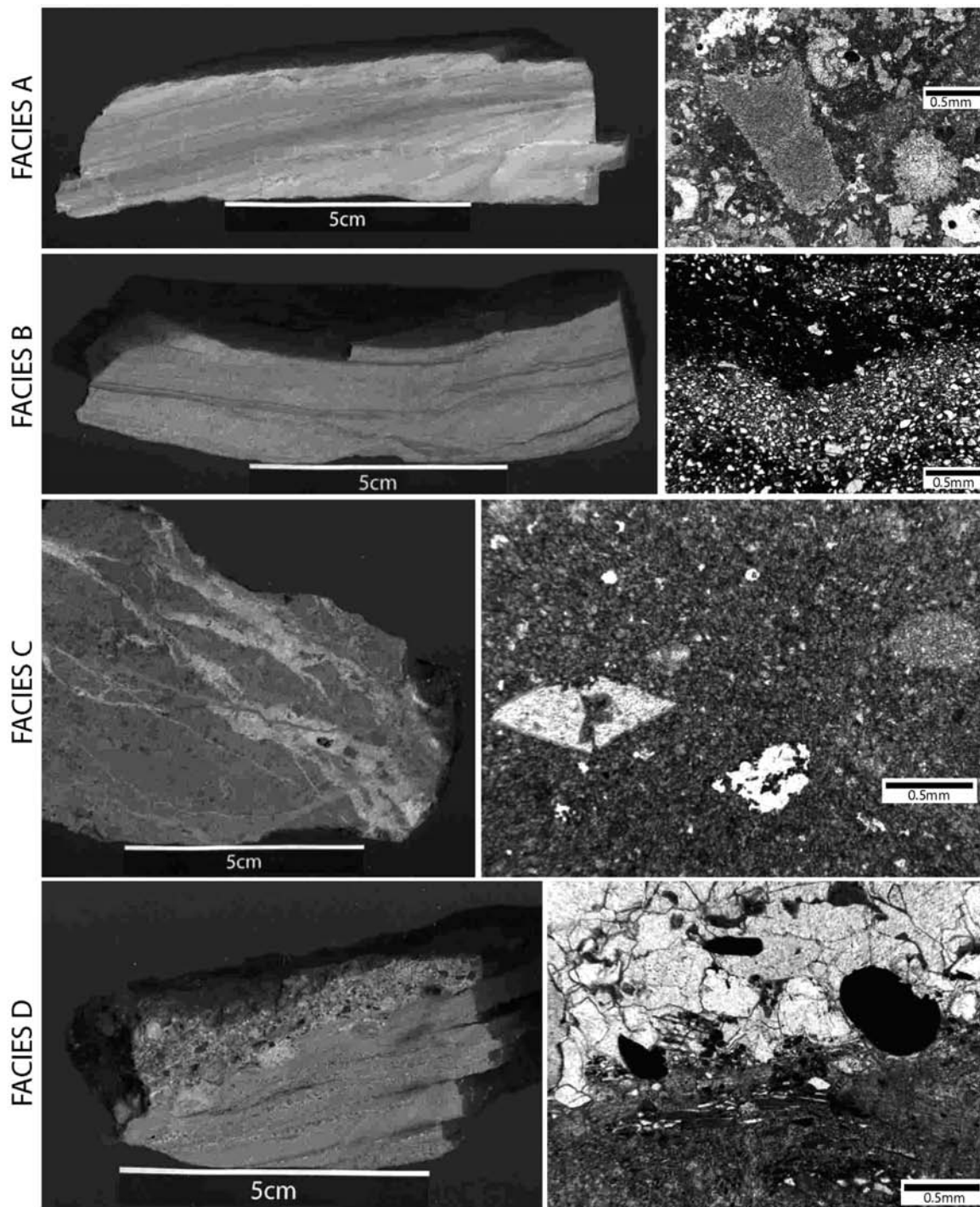


FIG. 5. – Macro and microfacies of karstic infillings. A) Polished rock slab of the facies A sample (left) and microphotograph (right) of a gray micrite rich in marine fauna: echinoderm and other invertebrate fossil fragments; B) polish rock slab of the facies B sample (left) and microphotograph (right) of a sandstone composed of grains of calcite, quartz and Fe-oxides nodules; C) polished rock slab of the facies C sample (left) and microphotograph (right) of ochre-orange microsparite reworking calcite grains, micritized grains and fossil ghosts; D) polished rock slab of the facies D sample (left) and microphotograph (right) of two infilling sequences, fine grain sediment including calcite, quartz, Fe-oxide nodules and biotite derived from the erosion of Cévennes schists (lower sequence) and the same material into fresh calcite spar (upper sequence).

FIG. 5. – Macro et microfaciès des remplissages karstiques. A) Face polie d'un échantillon de facies A (gauche) et microphotographie (droite) d'une micrite grise riche en faune marine : échinodermes et autres fragments de fossiles invertébrés ; B) face polie d'un échantillon de facies B (gauche) et microphotographie (droite) d'un grès composé de grains de calcite, de quartz et de nodules d'oxydes de fer ; C) face polie d'un échantillon de facies C (gauche) et microphotographie (droite) d'une microsparite orange-ocre remaniant des grains de calcite et de micrite ainsi que des fantômes de fossiles ; D) face polie d'un échantillon de facies D (gauche) et microphotographie (droite) de deux séquences de remplissage, d'un sédiment à grains fins contenant de la calcite, du quartz, des nodules d'oxydes de fer et de la biotite venant de l'érosion des schistes des Cévennes (séquences du bas) ainsi que le même matériel mélangé à de la sparite (séquence du haut).

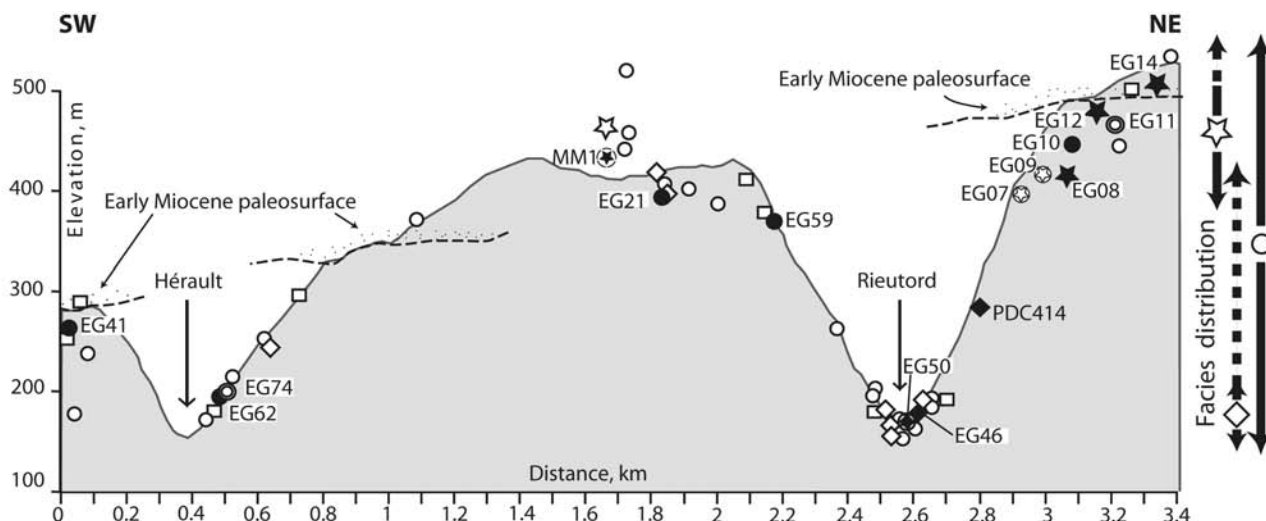


FIG. 6. – Location of the studied samples, projected onto a SW-NE section (location on fig. 2). The section is normal to the strike of the SE-dipping Jurassic strata, which are not represented. Arrows on the right indicate the extent of vertical facies distribution. Facies A samples (stars) is only found in the upper part of the massif, above 400 m in altitude. Facies B samples (diamonds) are mostly exposed in the lower 100 m of the canyon, with rare exceptions found higher (= 400 m in altitude). Facies C samples (circles) is found across the whole thickness of the massif. The Early Miocene alluvial deposits are represented on the perched paleosurfaces, along with Miocene to Present karsts cavities infill (squares) in the massif. The additional key for the symbols corresponding to age determination (and possible reworking), is provided in the text and accompanying figure 8b.

FIG. 6. – Localisation des échantillons étudiés, projetés sur une coupe SW-NE (située fig. 2). La coupe est perpendiculaire au pendage SE de la formation Jurassique, qui n'est pas représenté. Les flèches sur la droite indiquent la répartition verticale des faciès. Le faciès A (étoile) est observé uniquement sur les parties hautes du massif, au-dessus de 400 m d'altitude. Le faciès B (losange) se trouve essentiellement dans les 100 premiers mètres de hauteur des canyons, avec de rares échantillons trouvés plus haut (= à 400 m d'altitude). Le faciès C (cercle) est réparti de manière homogène sur l'ensemble du massif. Les dépôts d'alluvions du Miocène inférieur sont représentés sur des paléo-surfaces perchées, correspondant aux remplissages karstiques miocènes (carré) au sein du massif. Les variantes des symboles correspondent à l'âge des échantillons qui est fourni dans le texte et la figure 8b.

finer bivalve shells and numerous other shell fragments (fig. 7). Paleontology points to three distinct ages for this facies: Jurassic, Cretaceous and Paleocene (fig. 8).

The Jurassic age is given by *Aptychus* of Cephalopods [Lucas *et al.*, 1976]; more specifically, the presence of “microfilaments” allows to assign the first karstic infilling to the Late Jurassic (fig. 7, fig. 8). The Mid-Late Paleocene age is supported by the presence of both planktonic foraminifera and nannofossils (fig. 7, fig. 8a). *Sphenolithus* taxa (i.e., *Sphenolithus primus*) were recorded. In the GSSP (Global Boundary Stratotype Section and Point) of the Selandian Stage, placed at Zumaia (N Spain), the first rare occurrence of the *Sphenolithus* genus was recorded in the middle part of the Chron C27n, while its first continuous occurrence is situated towards the lower part of the Chron C26r [Bernaola *et al.*, 2009], being a latest Danian event. Few Cretaceous taxa were also identified in MM1 sample, Cretaceous nannofossils are found together with the Paleocene ones, being most probably reworked.

#### Facies B (diamonds in fig. 6 and 8)

The samples of Facies B show a horizontal internal lamination; they consist of very fine laminated sandstones, with colors ranging from beige to red. The bedding is highlighted by a variable content of iron oxi-hydroxides or sometimes by different concentrations of quartz grains (fig. 5). The infilling is a mixture of microsparite, quartz grains (whose content varies from 10 to 50%) and minor amounts of iron oxi-hydroxides. Facies B is also characterized by cross-lamination and disrupted laminae, which

suggests a significant depositional energy. Facies B samples are found in the lower part of the canyons, at an altitude less than 100 m above the present river level (fig. 6).

Some thin sections of facies B samples reveal planktonic foraminifera and nannofossils (fig. 7), which confirm their marine origin and provide a Paleocene age (fig. 8). The Paleocene identified calcareous nannofossil taxa indicate the presence of NP4 biozone of Martini zonation [1971], whose base is defined by the first occurrence of *Ellipsolithus macellus* (EG50 sample, fig. 8a). The genus *Fasciculithus* occurs in most of the Paleocene investigated samples. The recorded specimens are poorly preserved, hindering specific determination; only a few specimens could be assigned to the species *Fasciculithus ulii*, in EG50 sample, whose first occurrence is placed in the Latest Danian, slightly below the Danian/Selandian boundary [Tremolada *et al.*, 2008; Bernaola *et al.*, 2009]. A number of nannofossils found in Facies B are moderately preserved, with diagenetic overprint and/or dissolution; some of these yielded (Late) Cretaceous ages suggesting reworking and mixing with Paleocene nannofloras (fig. 8).

#### Facies C (circles in fig. 6 and 8)

The very heterogeneous facies C is prevalent in the studied area and is uniformly found across the whole depth of the canyon (fig. 6). It consists of a red-orange microsparite due to the presence of disseminated iron oxi-hydroxides. The sediment is often strongly recrystallized and sometimes includes scattered quartz grains or fragments of speleothems (fig. 5). A general feature of facies C is the presence of

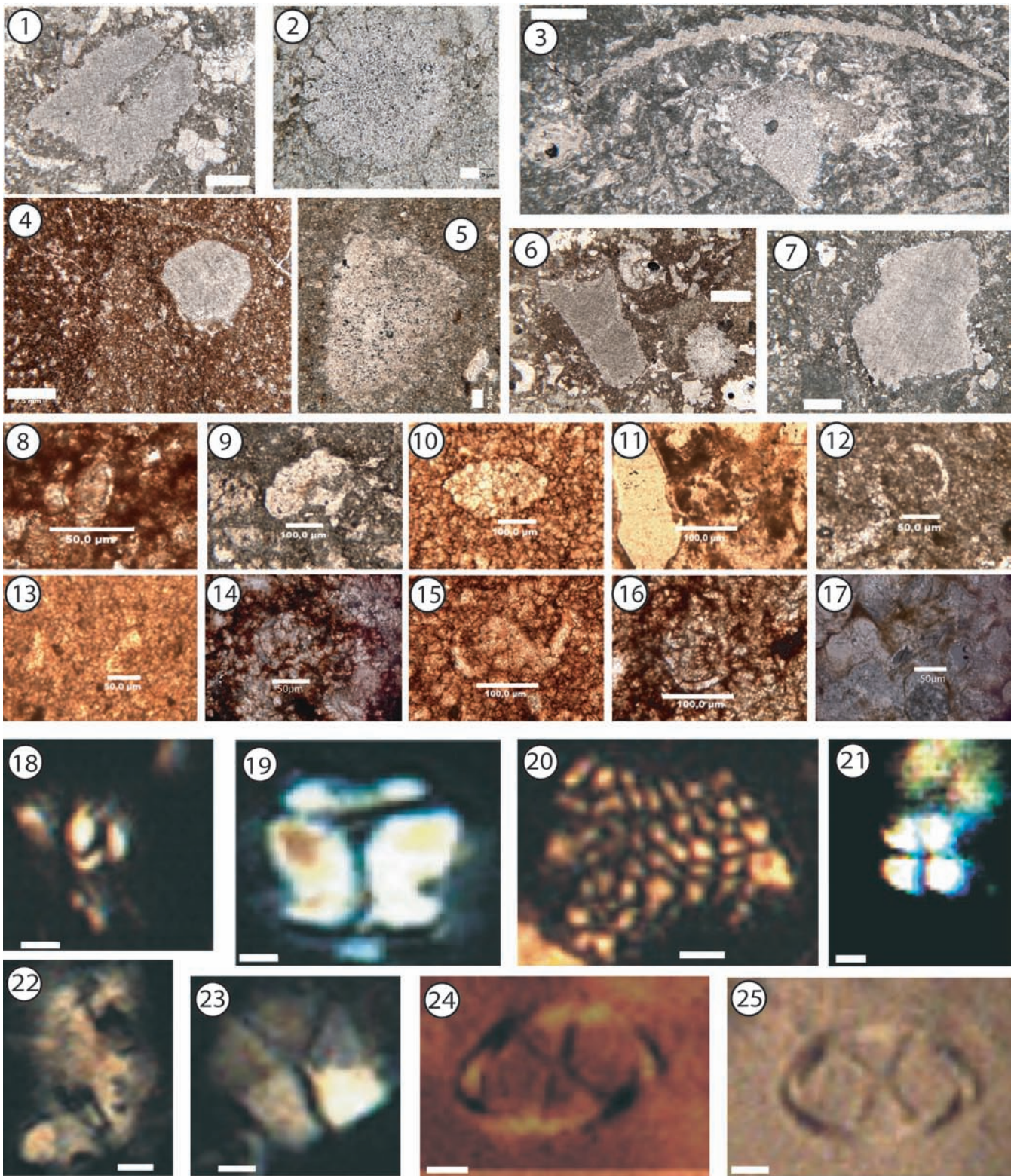


FIG. 7. – Paleontological remains: foraminifera and calcareous nannofossils from karstic infillings. 1-6: marine fossils such as : 1) cross section of echinoderm columnals from EG10 sample scale bar (SB) = 0.5 mm; 2) echinoid spine from EG14 sample, SB = 50  $\mu$ m; 3) aptychus from EG7, SB = 0.5mm; 4, 5, 6, 7: cross section of echinoderm from respectively EG 53, EG2, EG12 and EG14, SB4, 6, 7 = 0.5 mm, SB5 = 50  $\mu$ m ; 8-17: planktonic foraminifera such as: 8) *Praemurica cf. uncinata* (BOLLI) from EG59, SB = 50  $\mu$ m; 9) *Eoglobigerina spiralis* (BOLLI) from EG14, SB = 100  $\mu$ m; 10) *Igorina pusilla* (BOLLI) from EG62, SB = 100  $\mu$ m; 11) *Globanomalina imitata* (SUBBOTINA) from EG46, SB = 100  $\mu$ m; 12) *Acarinina strabocella* (LOEBLICH & TAPPAN) from EG8, SB = 50  $\mu$ m; 13) *Morozovella angulata* (WHITE) from MM1, SB = 50  $\mu$ m; 14) *Globanomalina ehrenbergi* (BOLLI) from EG62, SB = 50  $\mu$ m; 15) *Parasubbotina variospira* (BELFORD) from EG62, SB = 100  $\mu$ m; 16) *Subbotina triloculinoides* (PLUMMER) from EG59, SB = 100  $\mu$ m; 17) *Igorina tadjikistanensis* (BYKOVA) from PCD414, SB = 50  $\mu$ m ; 18-25: calcareous nannofossils all come from EG10 sample, SB = 1  $\mu$ m, such as: 18) *Prinsius martinii* (PERCH-NIELSEN, 1969) HAQ, 1971; 19) *Fasciculithus* sp.; 20) *Thoracosphaera* sp.; 21) *Sphenolithus primus* PERCH-NIELSEN, 1971; 22) *Ellipsolithus macellus* (BRAMLETTE & SULLIVAN, 1961) SULLIVAN, 1964; 23) *Braarudosphaera bigelowii* (GRAN & BRAARUD, 1935; DEFLANDRE, 1947); 24, 25) *Neochiastozygus cf. perfectus* PERCH-NIELSEN, 1971.

FIG. 7. – Faune, microfaune et nannofossiles calcaires des remplissages karstiques. 1-7 : fossiles marins ; 8-17 : foraminifères planctoniques ; 18-25 : nannofossiles calcaires.

disrupted laminae and /or the occurrence of micro-breccias (fig. 5) suggesting some depositional energy.

Unfortunately, most samples are undated, however some of them yield foraminifera and nannofossils, both poorly preserved (fig. 7), which provide Paleocene and Cretaceous ages, thus suggesting reworking (fig. 8). So far, no mixing between these 2 ages has been found within a single sample. *Neochiastozygus perfectus* rarely occurs in the studied samples (i.e., in the sample EG10, fig. 8a) characterizing the latest Danian. Cretaceous assemblages are clearly dominated by *Watznaueria barnesiae*, which represents over 60-70% of total nannofloras (EG11 and EG74). This species is one of the Cretaceous nannofossils most resistant to dissolution and diagenesis, therefore assemblages containing more than 40% of its specimens are considered as heavily altered [Roth and Krumbach, 1986].

### Facies D (squares in fig. 6)

The karstic infilling Facies D corresponds to laminated sandstones and micro-conglomerates with the presence of quartz pebbles, fragments of iron-rich lateritic crusts and distinctive clasts of schists (fig. 5) whose source can be identified in the Paleozoic metamorphic basement of the Cevennes, which crops out in the upper reaches of the present drainage area. No fossils or microfossils have been found in these karstic sediments, thus supporting a continental origin. The lithological composition of this karstic infilling is similar to residual conglomerates found on more recent paleosurfaces [Séranne *et al.*, 2002; Camus, 2003]. These detrital deposits include rounded cobbles and pebbles of quartz and sub-angular quartz exudates with schist fragments inclusions, derived from the sill or dike walls, mixed with oxidized silts. These deposits have been mapped from the upstream Cevennes high in the north, to the littoral plain of the Mediterranean sea in the south [Séranne *et al.*, 2002]. They are interpreted as remains of alluvial sediments of a south-flowing drainage, that post-dates the rifting of the Western Mediterranean realm (Oligocene-Aquitainian), once the regional direction of flow had been directed towards the newly formed NW Mediterranean sea [Séranne *et al.*, 1995]. In the studied area, this alluvial formation, derived from the erosion of the Cevennes, is found on presently perched paleosurfaces (fig. 6), disconnected by later incision of the river network that occurred in the Serravallian-Tortonian interval [Séranne *et al.*, 2002]. It represents a fluvial-alluvial surface deposit, while the similar karstic infill (Facies D) signs the underground karstic flow.

These episodes of karstification-infilling can be correlated with the structural field observations. The cavities whose infilling is parallel to the bedding of the calcareous host rocks, are dated Late Jurassic. Horizontal fillings, later than the regional tilting and earlier than the intra-Eocene "Pyrenean" orogeny, are dated Paleocene. Finally, horizontal infillings superimposed onto Pyrenean-related structures correspond to an Early Miocene to Present episode.

### Interpretation

Facies A, being found in two distinct structural settings (pre-tilting as well as post-tilting of the host rock) and bearing three distinct biostratigraphic markers (Jurassic, Cretaceous and Paleocene for Facies A), indicates that

facies distribution does not depend on the age of the marine event.

This **Facies A** is devoid of hydrodynamic structures, which suggests a depositional environment dominated by settling. It is often rich in marine shell debris and may contain fine detrital allochthonous clasts. This lithology suggests that the karstified area was entirely submerged by the sea and that the karst system was mostly filled by introduction of marine water and consequently, marine sediments. The distribution of Facies A in the area is restricted to the upper parts of the canyons, above an altitude of 400 m (fig. 6). This fact suggests that the deposition of Facies A sediments occurred over the epikarst paleotopography, characterized by sinkholes and pinnacles; they may have been introduced in the karstic network.

In spite of a similar macroscopic facies, Late Jurassic markers have never been found together with a dated Cretaceous or Paleocene marine content. This suggests that the marine Jurassic infilling sequence was followed by a period of lithification of the internal karstic sediment preventing reworking during the following karstification-infilling events. In addition, Jurassic infillings are characterized by one single facies : Facies A. Karsts filled by Jurassic marine sediments are found in very rare occurrences, only on the east bank of Rieutord, at an altitude higher than 400 meters. It is unclear whether karst at this elevation in the area indicates emersion surfaces related to high-frequency, low-amplitude sea-level changes during the deposition of shallow carbonate platform, during the Late Jurassic, or if they are the remains of one karstification stage that occurred at the end of the Late Jurassic. Indeed, the present erosional surface prevents us from asserting the amount of overlying calcareous formations that were karstified during this episode. In the absence of sufficient information, these Jurassic infillings will not be interpreted thereafter in terms of base level variation.

Unlike Jurassic fossils, Cretaceous markers have only been found as poorly preserved, reworked nannofossils, sometimes associated with various Paleocene markers. This suggests the reworking of marine Cretaceous sediments during the Paleocene marine event and mixing between the two age markers. However, the majority of Facies A samples yield only Paleocene taxa, without any evidence of reworking.

In contrast with Facies A, **Facies C** is a typical continental karstic sediment, resulting from strictly karstic hydrodynamics. Facies C is an undifferentiated karstic sediment which was deposited when the area was above the base level and was submitted to karstification. The lack of biostratigraphic markers in most Facies C samples prevents attributing an age to this facies. However, the presence of planktonic foraminifera and nannofossils in some samples accounts for reworking of marine sediments previously deposited in the karstic cavities or in subsurface. In this case, Facies C containing Cretaceous taxa was deposited after the marine Cretaceous event; it reworked marine sediments during the later karstification stages. Facies C containing Paleocene species was deposited after the marine Paleocene event and reworked marine sediments during a later karstification stage.

**Facies B** is characterized by: i) the generalized presence of quartz and iron oxy-hydroxide clasts, indicating a detrital

source from outside of the calcareous area, and by : ii) disrupted laminae in the sediment, recording the hydrodynamics of the karst system. This suggests energy and sediment

transport and deposition, typical of continental karstic sediments. However, the occurrence of planktonic foraminifera within the sediment suggests that at least part of the infill,

Sample	Marine content	Zones	Age of karstic filling	Symbol
	<b>Facies A</b>			★
EG7	Aptychus, microfilaments		Late Jurassic	★
EG9	Aptychus, microfilaments		Late Jurassic	★
EG8	Foram : <i>Acarinina strabocella</i> (LOEBLICH & TAPPAN)	P3a-P4a	Selandian-Thanetian	★
EG12	Foram : <i>Praemurica cf. uncinata</i> (BOLLI)	P2-P3 (basal part)	Dano-Selandian	★
EG14	Foram : <i>Eoglobigerina spiralis</i> (BOLLI)	P2-P3a; uppermost P1c	Dano-Selandian	★
MM1	Foram : <i>Morozovella angulata</i> (WHITE) Nanno : <i>Prinsius bisulcus</i> (STRADNER, 1963) HAY & MOHLER, 1967; <i>Fasciculithus</i> sp., <i>Markalius inversus</i> (DEFLANDRE in DEFLANDRE and FERT, 1954) BRAMLETTE & MARTINI, 1964; <i>Braarudosphaera bigelowii</i> (GRAN & BRAARUD, 1935) DEFLANDRE, 1947; <i>Thoracosphaera</i> sp.; <i>Sphenolithus primus</i> PERCH-NIELSEN, 1971	P3a-lower-mid P4 Biozone: N4 of Martini's Zonation (1971)	Selandian-	●
	<i>Watznaueria barnesiae</i> (BLACK in BLACK & BARNES, 1959) PERCH-NIELSEN, 1968; <i>Zeughrabdodus erectus</i> (DEFLANDRE in DEFLANDRE & FERT 1954) REINHARDT, 1965; <i>Retecapsa angustiforata</i> BLACK, 1971; <i>Micula decussate</i> VEKSHINA, 1959		Cretaceous most probably reworked	
	<b>Facies B</b>			◇
PDC414	Foram : <i>Igorina tadjikistanensis</i> (BYKOVA)	P3b-P5	Selandian-Thanetian	◇
EG46	Foram : <i>Globanomalina imitata</i> (SUBBOTINA)	P1b-P6	Danian-Selandian-Thanetian	◇
EG50	Nanno : <i>Ellipsolithus macellus</i> (BRAMLETTE & SULLIVAN, 1961) SULLIVAN, 1964; <i>Cruciplacolithus primus</i> PERCH-NIELSEN, 1977; <i>Sphenolithus primus</i> PERCH-NIELSEN, 1971; <i>Fasciculithus</i> sp.; <i>Fasciculithus ulii</i> PERCH-NIELSEN, 1971; <i>Chiasmolithus danicus</i> BROTZEN, 1959) HAY & MOHLER; <i>Thoracosphaera saxea</i> STRADNER, 1961; <i>Braarudosphaera bigelowii</i> (GRAN & BRAARUD, 1935) DEFLANDRE, 1947; <i>Markalius inversus</i> (DEFLANDRE in DEFLANDRE and FERT, 1954) BRAMLETTE & MARTINI, 1964; <i>Toweius pertusus</i> (SULLIVAN, 1965) ROMEIN, 1979	Biozone NP4 of Martini's Zonation (1971)	Late Danian-Early Selandian.	●
	<i>Watznaueria barnesiae</i> (BLACK in BLACK & BARNES, 1959) PERCH-NIELSEN, 1968; <i>Micula decussate</i> VEKSHINA, 1959; <i>Gartnerago segmentatum</i> (STOVER 1966) THIERSTEIN, 1974; <i>Arkhangelskiella cymbiformis</i> VEKSHINA 1959		Cretaceous most probably reworked	
	<b>Facies C</b>			○
EG10	Nanno : <i>Sphenolithus primus</i> PERCH-NIELSEN, 1971; <i>Neochiastozygus perfectus</i> PERCH-NIELSEN, 1971; <i>Prinsius cf. martini</i> , <i>Ellipsolithus macellus</i> (BRAMLETTE & SULLIVAN, 1961) SULLIVAN, 1964; <i>Toweius</i> sp.; <i>Fasciculithus</i> sp.; <i>Braarudosphaera bigelowii</i> (GRAN & BRAARUD, 1935) DEFLANDRE, 1947; <i>Thoracosphaera</i> sp.	Biozone: N4 of Martini's Zonation (1971)	Late Danian-Early Selandian.	●
EG11	Nanno : <i>Watznaueria barnesiae</i> (BLACK in BLACK & BARNES, 1959) PERCH-NIELSEN, 1968; <i>Staurolithites crux</i> (DEFLANDRE & FERT, 1954) CARATINI, 1963; <i>Micula decussata</i> VEKSHINA, 1959; <i>Arkhangelskiella cymbiformis</i> VEKSHINA 1959; <i>Lithraphidites quadratus</i> BRAMLETTE & MARTINI 1964; <i>Micula praemurus</i> (BUKRY 1973) STRADNER & STEINMETZ, 1984		Maastrichtian most probably reworked	○
EG21	Foram : <i>Igorina pusilla</i> (BOLLI)	P3-P4 (lower part)	Selandian	●
EG41	Foram : <i>Morozovella angulata</i> (WHITE)	P3a-lower-mid P4	Selandian-Thanetian	●
EG59	Foram : <i>Subbotina triloculinoides</i> (PLUMMER), <i>Praemurica cf. uncinata</i> (BOLLI)	P1b-P4 P2-P3 (basal part)	Late Danian-Early Selandian.	●
	Foram : <i>Parasubbotina variospira</i> (BELFORD), <i>Globanomalina ehrenbergi</i> (BOLLI), <i>Igorina pusilla</i> (BOLLI)	P3a-P4 (lower part) P2-P4 P3-P4 (lower part)	Selandian	
EG 74	Nanno : <i>Watznaueria barnesiae</i> (BLACK in BLACK & BARNES, 1959) PERCH-NIELSEN, 1968; <i>Micula decussate</i> VEKSHINA, 1959		Cretaceous most probably reworked	○

FIG. 8a

	Undated	Jurassic (fossils)	Paleocene (Foram+Nanno)	Reworked Late Cretaceous (Nannofossils)	Miocene to present me (detrital source)
Facies A	★	●	★	●	
Facies B	◇		◇	●	
Facies C	○		●	○	
Facies D					□

FIG. 8b

FIG. 8. – Synthesis of age control: a) paleontological content of facies A (stars), B (diamonds) and C (circles), distinguishing in situ from reworked fossils (combination of symbols); b) interpretative key for the figure 8a, as well as for figures 2, 6 and 9.

FIG. 8. – Synthèse chronologique ; a) contenu paléontologique des différents faciès A (étoiles), B (losanges) et C (cercles), et distinguant les fossiles in situ des fossiles remaniés ; b) interprétation de la figure 8a avec les symboles utilisés dans les figures 2, 6 et 9.

Calcareous nannofossils taxa references / Références des nannofossiles calcaires.

most probably reworked, results from marine flooding in karstic cavities located below sea-level. Such a mix between continental karstic and marine karstic dynamics, strongly suggests a coastal environment [Bruxelles *et al.*, 1999; Camus, 2003] subjected to emersion-submersion cycles, including reworking of submersion-related marine karstic sediments into the emersion-related continental karstic sediments. Facies B represents an intermediate between Facies A in the marine domain and Facies C in the totally continental domain. Paleocene nannofossils have been found in the samples of Facies B, in association with reworked Cretaceous taxa, and some samples have only yielded Paleocene foraminifera. No samples yielded exclusively Cretaceous taxa. This suggests that the Facies B was only deposited during the Paleocene transgression and that it may rework some marine Cretaceous sediments.

Facies A, B and C contain Cretaceous and Paleocene marine taxa, indicating two marine events. These marine episodes are distinct because: i) Cretaceous taxa are always found in a poor state of preservation, which suggests a strong reworking during a subsequent karstification phase and ii) reworked Cretaceous taxa have been found associated with Paleocene taxa in Facies A, which is an original undisturbed laminated facies deposited by settling. It shows that marine Cretaceous sediments were reworked during Paleocene times.

**Facies D** signs a more recent continental (karst and alluvial) depositional episode that took place from the Early Miocene [Séranne *et al.*, 2002]. Due to the long time interval between the Paleocene karst episodes and this later event and also due to the lack of precise biostratigraphic markers to characterize its evolution, it was not possible to integrate it in the interpretation in terms of base-level evolution. Therefore, in the following, we restrict the interpretation to the Late Cretaceous-Paleocene event.

#### SCENARIO OF FACIES DISTRIBUTION FOR MARINE LATE CRETACEOUS AND PALEOCENE EVENTS

Northwest of the studied area, small and highly discontinuous outcrops of shallow marine sediments dated from Turonian-Santonian (with coastal Turonian facies), then marine Coniacian deposits followed by lacustrine Campanian-Maastrichtian deposits [Alabouvette *et al.*, 1984, 1988; Bruxelles *et al.*, 1999] are exposed. In addition, southeast of the studied area, the presence of a Campanian marine fauna [Alabouvette *et al.*, 1988] suggests that the base level of the region was close to the sea level throughout the Late Cretaceous. With the onset of Maastrichtian lacustrine facies, the base level was lowered. The marine Cretaceous sediments found in karstic infilling in the studied area correspond to this Late Cretaceous marine event, which affects the whole region.

The karstification event that created the cavities, subsequently filled with Paleocene and reworked Cretaceous sediments, took place between the Late Cretaceous (Campanian) and Paleocene (Danian-Selandian) marine episodes, i.e. during the Maastrichtian-earliest Paleocene interval, related to the latest Cretaceous episode of the Pyrenean tectonics [Combes *et al.*, 2007].

We propose the following sequence for the Late Cretaceous-Paleocene event, which accounts for the facies and age distribution (fig. 9):

1– during Late Cretaceous times (Turonian to Maastrichtian), marine sediments are deposited across the studied area [Alabouvette *et al.*, 1984; 1988; Bruxelles *et al.*, 1999];

2– the Maastrichtian lacustrine sedimentation in the tabular “Grands Causses” and the continental fluvio-lacustrine sedimentation of “Rognacian” (Upper Maastrichtian) and “Vitrollian” (Danian) facies in the south of the study area [Freytet, 1970; Freytet and Plaziat, 1982], show a lowered base level and indicate a continental environment. Aerially exposed carbonates were submitted to karstification and earlier marine deposits (Turonian-Maastrichtian) were weathered and reworked into the new karstic cavities. This period of karstification spans the Maastrichtian through to the Late Danian transgression. The karstic sediments include reworked marine Late Cretaceous taxa within the Facies C deposits, which contain Cretaceous nannofossils only;

3– during the initial stages (Late Danian) of the following transgression, coastal environments around the calcareous area record the contribution of both marine and karstic dynamics, with deposition of continental as well as marine sediments found in the Paleocene Facies B. During this phase, the reworking of Cretaceous sediments continued and may have also incorporated Cretaceous taxa into Facies B sediments of Paleocene age;

4– during the maximum of Paleocene transgression, the base-level rose above the highest karst cavities across the entire study area. Settling of marine sediments of Paleocene Facies A, which may also incorporate remains of marine Late Cretaceous sedimentary cover, occurred in the karsts cavities;

5 – when the base level fell again, karstification processes resumed, and karstic dynamics reworked previously deposited marine sediments, including Paleocene and Late Cretaceous marine deposits. This induced deposition of Facies C sediments. Base level drops and rises during Late Cretaceous-Paleocene time interval are thus responsible for the present distribution of marine karstic sediments within the karstified massif (fig. 6).

#### QUANTIFICATION OF THE BASE LEVEL VARIATION DURING THE LATE CRETACEOUS-PALEOCENE EVENT

When the emersion and the submersion of a carbonate area can be documented by karstification and infilling by marine sediments, it becomes easier to quantify the magnitude of the variation of the corresponding base level. For the Cretaceous-Paleocene event, cavities containing dated infillings allow to quantify the amplitude of variation of this base level. There are marine Paleocene sedimentary fillings spread over the entire height of the massif, from the lowest parts (river-level) to the highest crests. This means that the pre-filling karstification has affected the entire height of the area, at least down to the present riverbed, to form the karst system. Then, during the following marine transgression, marine sediments gradually filled the cavities. The massif is

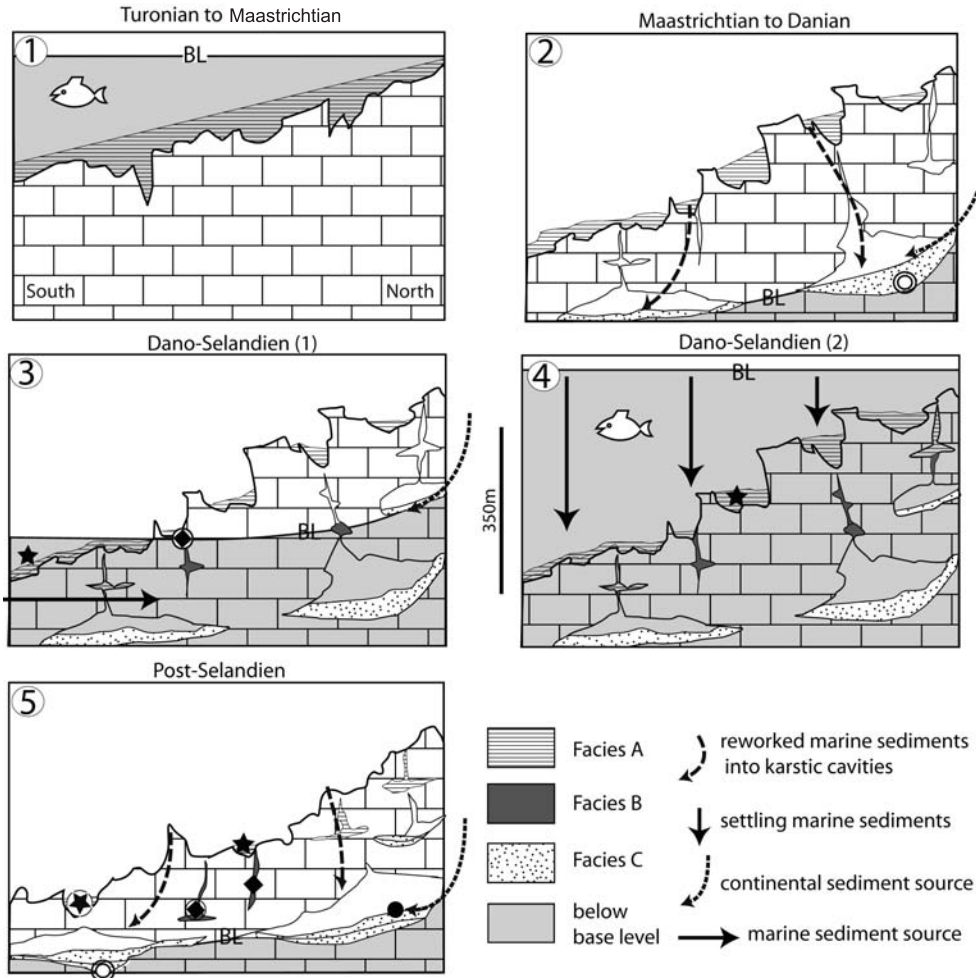


FIG. 9. – Simplified scenario of the Late Cretaceous - Early Paleocene karstification - marine transgression: 1) Marine Late Cretaceous sediments are deposited on the Jurassic carbonates, eroded and karstified during Mid-Cretaceous time; 2) lowering of base level results in subaerial exposure of the Jurassic limestones and their sedimentary cover; this induces weathering then deposition of reworked late Cretaceous marine sediment in the enlarging karst cavities; 3) base level rise induces transgression and development of coastal environments, mixing karstic dynamics (reworking Late Cretaceous sediment) and marine dynamics (supplying Paleocene taxa) within the karstic network, typical of facies B; 4) when the massif is completely submerged, karstic dynamics is stopped within the cavities, where deposition is controlled by settling, such as in facies A; 5) base level drop leads to a new emersion that exposes again the Jurassic limestones to weathering and karstification. Sediments deposited as facies C including Paleocene reworked taxa. Facies symbols as in figure 8; from stage 1 to 4, symbols represent only the facies deposited during this stage, whereas stage 5 represents the final facies distribution. BL= base level.

FIG. 9. – Scénario de la karstification-transgression marine de la fin du Crétacé-début du Paléocène. 1) Les sédiments marins de la fin du Crétacé se sont déposés sur les carbonates du Jurassique érodés et karstifiés durant la période du Crétacé "moyen"; 2) la baisse du niveau de base expose les calcaires jurassiques à la karstification et la couverture sédimentaire à l'érosion, induisant l'altération puis le dépôt des sédiments crétacés marins remaniés, dans de nouvelles cavités karstiques; 3) la remontée du niveau de base induit une transgression et le développement d'un environnement littoral, combinant la dynamique karstique (remaniant des sédiments crétacés) et l'apport marin (introduction de taxons paléocènes) dans le réseau karstique, témoignant du faciès B; 4) quand le massif est totalement submergé, la dynamique karstique cesse de fonctionner dans le réseau où le dépôt n'est plus contrôlé que par la décantation, comme en témoigne le faciès A; 5) la baisse du niveau de base conduit à une nouvelle émergence, qui expose une fois de plus la plateforme carbonatée jurassique à l'altération et la karstification. Les sédiments marins précédemment piégés dans le karst sont remaniés et redéposés sous la forme du faciès C incluant des taxons paléocènes remaniés. Les symboles des faciès de la figure 8 représentent le faciès déposé pendant la période donnée pour les stades 1 à 4, et la distribution finale des faciès pour le 5<sup>ème</sup> stade. BL = niveau de base.

above the base level when karstification occurs and below base level when marine sediments fill it.

The base level drop is at least 350 m in amplitude, which is the vertical extent of the observed a karst in the exposed area. This is a minimal value, as it does not consider the possible occurrence of a karst network below the riverbed. In a second phase, during Danian-Selandian times, the massif was completely submerged because marine sediments have been found at the top of the area. The amplitude of the

base-level rise is 350 meters minimum. Again, this is a minimal value, as a possible erosion of the carbonate formations at the top of calcareous area, and the bathymetry during Paleocene transgression are not taken into account. Indeed, the uppermost outcrops that have yielded marine fauna are intrakarstic cavities, which implies up to several tens of meters thickness of limestones that have been eroded and an additional several tens of meter of bathymetry above the present erosional surface are likely.

**DISCUSSION: THE POSSIBLE CAUSES OF HIGH-AMPLITUDE BASE LEVEL CHANGES**

**Eustatic forcing?**

The onshore record of base level variations due to eustasy requires global oscillations of the sea-level of similar amplitude, during the considered time interval. The observed polyphase karst evolution over the Latest Cretaceous to Early Paleocene interval suggests several events. The sea level curve of Kominz and others [2008] provides a chart with 0.1 Ma time resolution, showing the high frequency oscillations (fig. 10). We have shown that the amplitude of variation of the base level of 350 m occurred between the Late Maastrichtian and the Danian-Selandian. However, for the considered interval, this eustatic chart displays a maximum drop of 50 m between 65.4 and 63.8 Ma and a maximum rise of 52 m between 62 and 61.7 Ma (fig. 10), which is much less than the base level amplitude ( $\geq 350$  m) necessary to account for our observations.

However, the occurrence of foraminifera found in the study area, plotted on the biostratigraphic scale and eustatic

curve (fig. 10), reveals that the time interval [Wade *et al.*, 2011] of foraminifera found in the fillings overlaps the period of eustatic sea-level highs (Late Danian to Early Thanetian) following the eustatic lows of Maastrichtian to Early Danian. But the most restrictive time span common to all foraminifera found in the study area postdates the highest highstand, according to Kominz and others [2008]. In addition, two planktonic foraminifera species, *Praemurica uncinata* (stratigraphic interval according to Wade and others [2011]) [P2-P3a (basal part)] and *Igorina tadjikistanensis* [P3b-P5], found in the studied area are not contemporaneous. They occur respectively before and after the eustatic low stand between 61.1 Ma and 60 Ma (fig. 10). This supports polyphase events, with a first marine event in Late Danian, followed by a second marine event during Mid-Selandian, separated by an eustatic sea-level fall of several tens of meters, and associated subaerial exposure.

Although eustasy alone cannot account for base level changes observed in the study area, it appears to be related in some way to the distribution of marine markers within the karstified massif.

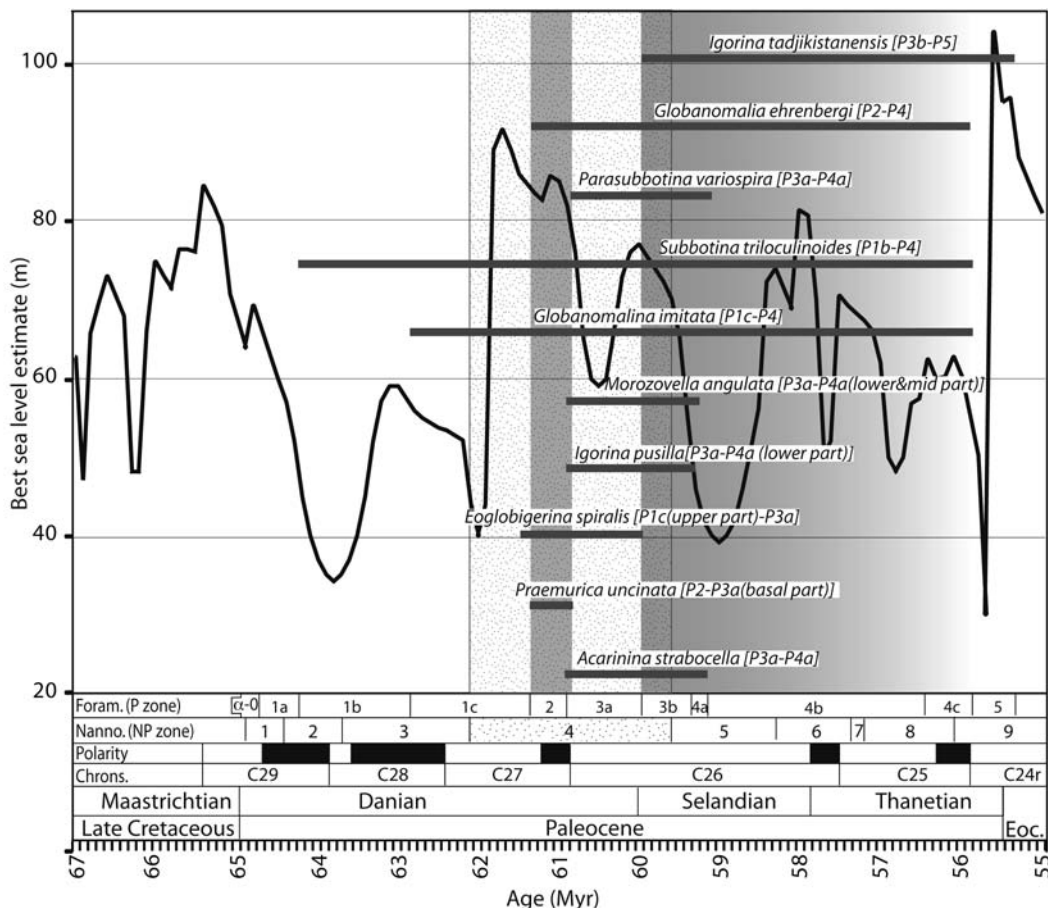


FIG. 10. – Eustatic curve of Kominz *et al.* [2008] superimposed onto the interval of occurrence of the foraminifera (horizontal bars) and of nannofossils (stippled area) found in the study area, according to references given in figure 8. Foraminiferal biozones from Wade *et al.* [2011] and nannofossil biozones from Miller *et al.* [2005] are calibrated on Cande and Kent [1995] time-scale. Note that since *Praemurica uncinata* and *Igorina tadjikistanensis* (grey shading) do not overlap, and are separated by an eustatic low. The younger boundary of the later interval is not constrained.

FIG. 10. – Occurrences des foraminifères (barres horizontales) et des nannofossiles (zone pointillée) trouvés dans la zone d'étude selon les références données dans figure 8, superposées sur la courbe eustatique de Kominz *et al.* [2008]. Les biozones de foraminifères de Wade *et al.* [2011] et de nannofossiles de Miller *et al.* [2005] sont calibrés sur l'échelle de temps de Cande et Kent [1995]. Notez que les périodes de vie des foraminifères *Praemurica uncinata* et *Igorina tadjikistanensis* (nuances de gris) ne se chevauchent pas et sont séparées par une baisse eustatique. La limite du dernier événement marin n'est pas contrainte.

### Geodynamics forcing?

The studied area (fig. 1) has undergone the Pyrenean orogeny from Latest Cretaceous to Middle Eocene [Philip *et al.*, 1978; Alabouvette and Cavelier, 1984; Arthaud and Laurent, 1995]. The Cévennes fault then acted as a left-lateral strike-slip, accommodating shortening of the Mesozoic cover on the southeastern bloc, expressed by a series of thrusts and anticlines in the Garrigues area [Séranne *et al.*, 1995], while the northwestern block remained mostly unaffected, except by minor brittle faulting [Demangeon, 1959; Alabouvette and Cavelier, 1984; Arthaud and Laurent, 1995]. Indeed the studied area, located northwest of the Cévennes fault, does not display any significant thrusts or faults. The lack of ramp cutting through the sedimentary cover prevents the development of significant hanging wall uplift. In addition, in the Languedoc between Pyrenees and Provence, the last major compressional phase occurred in Mid-Late Eocene [Philip *et al.*, 1978], which post-dates the recorded event. Considering that karstification and a flooding event occurred in the Latest Cretaceous – Early Paleocene time interval (i.e. several millions years), the inferred vertical movements would require rates of uplift and subsidence in the range of 0.1 mm per year. Such rates of uplift characterize zones of moderate tectonic activities [Pederson *et al.*, 2006]. The tabular structure of the area would indicate long-wave movements rather than differential vertical movement. Indeed, rates of uplift in plateaus [Binnie *et al.*, 2008] are compatible with the measured rate of base-level change. However, the evidence of polyphase karstification/flooding events during the Paleocene (fig. 10) requires faster rates of uplift and subsidence for smaller time intervals (less than one million year long). For the first marine event (61.3 to 60.8 m.y.), the required rate of subsidence would be close to 0.9 mm/yr. For the following interval (60.8 to 60 m.y.), the inferred rate of uplift would be around 0.5 mm/yr. Such values are documented in orogenic zones, characterized by intense deformation involving thrusting and folding, as well as denudation of the metamorphic basement [Fitzgerald *et al.*, 2005; Annen and Scaillet, 2006; Champagnac *et al.*, 2009; Norton *et al.*, 2011]. The studied area is clearly not tectonically affected to that extent. Finally, a sequence of subsidence immediately followed by uplift and subsidence again, each one of more than 350 meters amplitude, in a several millions-years-long interval, calls for an unknown geodynamic model. Such a “geodynamics yo-yo”, is therefore geologically unlikely.

### Hypothesis of a “dessiccated deep basin model” [Clauzon, 1982]

Eustasy and classical geodynamic models do not satisfactorily account for the 350 m amplitude of base level changes, especially during the early Paleocene base level oscillations.

Other examples of deep and fast erosion and karstification of carbonate massifs, not directly related to sea level change or geodynamics, have been already studied. The Messinian dessiccation of the Mediterranean Sea constitutes the most spectacular and well-documented example. In particular, the consequences of the Mediterranean base-level drop consecutive to its dessiccation, lead to the adaptation of the continental watershed [Clauzon, 1979;

Audra *et al.*, 2004; Camus *et al.*, 2004; Mocochain *et al.*, 2006; Bache *et al.*, 2011]. Unlike the drainage areas underlain with a terrigenous sedimentary cover, which were deeply eroded and incised by deep and narrow canyons (e.g. more than 1000 m beneath present coastline for the Rhône and the Nile rivers [Clauzon, 1982]), the response of the carbonate platforms surrounding the dessiccated area was dominated by fast and deep lowering of the karst system by dissolution of the limestone along conduits through the calcareous massif [Camus, 2003; Audra *et al.*, 2004; Clauzon *et al.*, 2005; Mocochain *et al.*, 2006]. In the present Mediterranean watershed, the deep underground karst systems, developed several hundred meters below the actual valleys and canyons [Camus, 2001; Gilli and Audra, 2004], as well as below present sea-level [Blavoux *et al.*, 2004] is accounted for by the sudden drop of the Mediterranean sea and the similarly fast adaptation to the new drainage profile between the hinterland and the residual dessiccated lake level, some 1700 m below pre-dessiccation sea-level [Clauzon *et al.*, 2005].

Such a geodynamic scenario involved karst development over hundreds of meters thickness in carbonate strata, followed, at the onset of Zanclean, by catastrophic flooding of the dessiccated endoreic basin [e.g. Bache *et al.*, 2011]. The underground karsts system previously formed through the marginal calcareous area were then flooded during the Zanclean refilling of the Mediterranean sea [Camus, 2003; Audra *et al.*, 2004 ; Mocochain *et al.*, 2006; Lofi *et al.*, 2011].

In order to account for the observed  $\geq 350$  m amplitude of the base-level variation during the Paleocene, we propose a scenario similar to the Messinian-Zanclean event that occurred in a silled endoreic basin. We hypothesize that the presence of Early Paleocene marine infilling in latest Cretaceous-Paleocene karst structures, developed at the expense of Peri-Tethyan Mesozoic carbonates of southern France, represents the geographical extent of the endoreic basin of Languedoc. Such outcrops have been previously mapped [Combes *et al.*, 2007]. They are bounded northward by the Paleozoic metamorphic basement. Southwards, they are covered by Oligocene to Neogene sequences, related to the rifting and opening of the NW-Mediterranean Sea. Although the southern margin is not known, it was located north of the Oligocene pre-rift position of the Paleozoic basement of Corsica and Sardinia. While the eastern margin is not precisely known, the western margin seems to extend along the present Pyrenean range. The location of the connection with the World Ocean is still debated. It could be through a narrow strait to the west [Peybernès *et al.*, 2001; Combes *et al.*, 2007, 2008].

When the sill is closed, the basin base-level is not controlled by eustasy anymore but by the balance between runoff in the watershed and evaporation of the water body in the axis of the endoreic Languedoc basin. Base-level develops from the bottom of the basin, upstream, and the karstification is initiated on the edges of the basin (fig. 11). When the sill becomes submerged, the World Ocean floods the basin. The base level of the basin is connected again with the World sea level, and marine sediments fill the karstic network previously formed (fig. 11).

The formation of the Languedoc endoreic basin occurred after the last marine Cretaceous deposit (Campanian)

and before the first marine deposit in Early Paleocene times (Late Danian), probably caused by geodynamic processes, mostly during the latest Cretaceous tectonic event. At that time, differential uplift of the Cevennes and Grands Causses relative to the Garrigues (fig. 1) [Séranne *et al.*, 2002] contributed to the formation of the Languedoc basin, with an upstream to the north and downstream to the south. During the formation of the Languedoc endoreic basin, base level dropped and was controlled by water bodies in the axis of the basin. So the  $\geq 350$  m base level drop indicates that the studied area was located to the north at least 350 meters above the altitude of the basin axis (fig. 11).

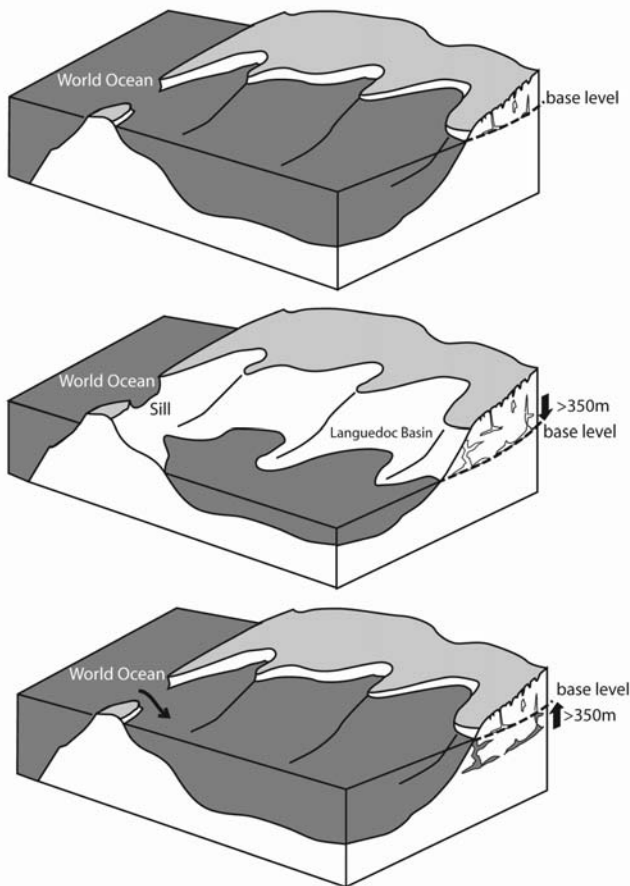


FIG. 11. – Conceptual sketch of the silled endoreic basin. A) Initial stage. B) A moderate eustatic fall disconnects the basin from the World Ocean. Evaporation induces local base level drop of the water body in the axis of the endoreic silled basin. In the study area, the base level drops of at least 350 m and the carbonate massifs located above the base level are karstified. C) A moderate eustatic rise induces submersion of the sill and flooding of the basin, and rise of the base level. The karstified carbonates are invaded with marine water and the cavities filled with marine sediments. The position of the sill is debated; it could be in the west, connecting with the Atlantic [Combes *et al.*, 2004, 2007].

FIG. 11. – Modèles 3D d'un bassin endoréique à seuil. A) Stade initial. B) Une baisse eustatique modérée peut déconnecter le bassin de l'Océan global. L'évaporation induit une chute du niveau de base jusqu'au fond du bassin endoréique. Ici, le niveau de base chute de 350 mètres au minimum et les massifs carbonatés se trouvant au-dessus de celui-ci sont karstifiés. C) Une faible remontée du niveau eustatique peut induire la submersion du seuil et l'envahissement du bassin, faisant remonter son niveau de base. Les parties carbonatées du massif sont alors envahies par la mer et les cavités du réseau piègent des sédiments marins. La position du seuil est encore débattue ; il pourrait être situé à l'ouest, connectant le bassin languedocien à l'Atlantique [Combes *et al.*, 2004, 2007].

The Early Paleocene marine sediments that filled the karstic network were deposited during the submersion of the sill and the flooding of the basin, when it was connected again with the World Ocean (fig. 10). The eustatic curve of Kominz and others [2008] displays a fast sea level rise, nearly 50 m amplitude, between 62 and 61.7 Ma, that may have allowed the World Ocean to submerge the sill (fig. 10). But, in the study area, there is no evidence of a Mid-Danian fauna (zone P1) related to a marine flooding due to the high-stand at 61.7 Ma. The record of the marine flooding is slightly delayed (61.3 Ma) with respect to the high-stand at 61.7 Ma (fig. 10). This could result from an incomplete sampling in our study, or from geodynamic interactions: in spite of the high-stand (61.7 Ma), the sill may have remained closed by thrusting; alternatively, the basin-floor in the studied area was undergoing uplift. Our observations further show the occurrence of at least two distinct and successive marine fillings: zone P2 and sub-zone P3b separated by a circa 20 m eustatic relative low. This supports a polyphase event, with a first flooding in Late Danian, followed by a second flooding during Early-Selandian (fig. 10). Similarly, the eustatic low at 59 Ma possibly involved an additional closure and dessiccation of the basin, although no supporting biostratigraphic markers were found in the study area. Interestingly, up to three marine intervals (from Mid-Danian to Selandian) have been identified west and south of the studied area [Combes *et al.*, 2004, 2007].

In any case, our results imply that the sill controlling the endoreic basin was extremely shallow. The amplitude of the eustatic change (several tens of meters, according to Kominz *et al.* [2008]) is indicative of the bathymetry of the sill that separated the Languedoc basin from the World Ocean. But it is likely that the sill was not a permanent structure in the convergent geodynamic context of the area, at that time. Thrusting must have exerted a long-term control on the sill geometry, while eustatic changes acted as the punctuated tempo of dessiccation/flooding of the endoreic basins. Indeed, the high stand at the Paleocene-Eocene boundary (fig. 10), is not recorded in the area by a marine transgression. Furthermore, the successive highstands that occurred during Ypresian and Lutetian, although more than 50 m higher than the previous Paleocene highstands [Kominz *et al.*, 2008], are not associated with marine flooding. On the opposite, the stratigraphic record has remained continental from that time onwards [Philip *et al.*, 1978; Freyret and Plaziat, 1982]: this suggests that Eocene tectonics had become the major control over the evolution of the studied area. The connection with the World Ocean was definitively closed and the entire endoreic basin was subjected to inversion and uplift due to the Pyrenean thrusting.

One significant difference with the Mediterranean Messinian-Zanclean model is the continental nature of the basin-floor basement for the Paleocene endoreic basin, whereas the Messinian event affected a much deeper oceanic-crust-floored basin. This implies moderate bathymetry and a base-level drop limited to several hundred meters. Another difference is the absence of evaporites expected to cover the basin floor of a dessiccated basin. However, the marginal position of the study area and the dominant continental character of the internal karstic sediments suggest that evaporites may have been deposited in the axis of the basin, south of the studied area. However, they have been

later subjected to inversion, uplift and erosion during the successive phases of the Pyrenean orogeny. Nevertheless, it should be noted that Paleocene marine evidences are found in karstified carbonate rocks that are locally dolomitized (see fig. 2). Such secondary dolomitization could tentatively be related to the occurrence of penesaline sea water during drying periods of the basin, without precipitation of evaporites [Qing *et al.*, 2001; Melim and Scholle, 2002]. In addition, the studied area displays sulfide Pb-Zn deposits [Le Strat, 1975] of indeterminate age. These accumulations show dolomite and karst breccia, similar to Paleocene facies, and we suggest that they may be associated with the desiccation and salinity increase [Wright and Wacey, 2005].

## CONCLUSION

Occurrence of marine sedimentary infilling in a karst system developed in a calcareous area, has already been documented in southern France [e.g. Peybernès *et al.*, 2003, Combes *et al.*, 2007]; however, our study quantifies the vertical extent of the phenomena and explores its geodynamic consequences. The karst development and its marine infill over more than 350 m in height, provides direct evidence of base-level changes of at least that amplitude. Foraminifera and nannofossils associated within the karstic sedimentary infilling constrain the age and duration of the process. The large amplitude and the fast rate of change of base-level cannot be accounted for by neither eustasy nor tectonics. We propose that variations of base-level were induced by desiccation/flooding cycles in a silled endoreic basin, extending across the south of France. The extent of such continental-crust-floored basin is difficult to delineate, due to the later Cenozoic Pyrenean thrusting and folding, then NW-Mediterranean rifting and drifting. During eustatic low-stand, the sill was exposed, the basin was disconnected

from the World Ocean, and the local Peri-Tethyan carbonates (Late Jurassic in age) were submitted to erosion and karstification down to the dropped base-level. When eustatic sea-level rose, the sill was submerged and the basin flooded; the karst was transgressed and marine sediments were trapped in the cavities. The model is similar to the later Messinian-Zanclean event that affected the whole Mediterranean, especially for the development of deep karsts in the carbonate-dominated platform. Our results suggest that it is likely that part of the deep karst systems described on the Mediterranean margins –and that are usually related to the Messinian-Zanclean event– have been initiated during the Paleocene, and reactivated during the Messinian (or later) event(s). However, we anticipate that differential geodynamic evolution of distinct calcareous massifs may have brought some of them below the Messinian dropped base-level – and therefore shielded them from Messinian karst reactivation. This could be the case for the hanging-wall of the extensional faults of the NW-Mediterranean rifting. On the opposite, blocks that have been uplifted above the base-level, within the hanging-wall of Pyrenean thrusts, must record both Paleocene and later karstification episodes.

Therefore paleokarsts record the variations of base-level, and this can be used to constrain the geodynamic evolution of continental areas otherwise devoid of stratigraphic record.

*Acknowledgments.* – This study was initiated with the financial support of INSU-CNRS and it is now part of a PhD (E.H.) sponsored by: “Projet Scientifique de l’Université Montpellier 2” and BRGM. The authors wish to thank Christophe Nevado and Doriane Delmas who have performed all the high quality thin sections, which were pivotal in this study. The paper was substantially improved by constructive reviews from J.-P. Suc and J. Vergés.

*SGF associate editor: Romain Augier*

## References

- ALABOUVETTE B., AZEMA C., BODEUR Y. & DEBRAND-PASSARD S. (1984). – Le Crétacé supérieur des Causses. – *Géol. France*, **1-2**, 67-73.
- ALABOUVETTE B., ARTHAUD F., BODEUR Y., PALOC H., SEGURET M., LE STRAT P., ELLENBERGER P., MACQUAR J.C. & COUMOUL A. (1988). – Carte géologique de la France au 1/50 000. Feuille du Vigan. – BRGM, Orléans.
- ALABOUVETTE B. & CAVELIER C. (1984). – Languedoc oriental, in Chapitre Paléogène. Synthèse géologique du Sud-Est de la France. *In*: S. DEBRAND-PASSARD & S. COURBOULEIX, Eds, Stratigraphie et paléogéographie. BRGM, Orléans, France. – *Mém. BRGM*, **125**, 434-438.
- ANNEN C. & SCAILLET B. (2006). – Thermal evolution of leucogranites in extensional faults; implications for Miocene denudation rates in the Himalaya. – *Geol. Soc. Sp. Publ.*, **268**, 309-326.
- ARTHAUD F. & LAURENT P. (1995). – Contraintes, déformation et déplacement dans l’avant-pays nord-pyrénéen du Languedoc méditerranéen. – *Geodin. Acta*, **8**, 142-157.
- ARTHAUD F. & SEGURET M. (1981). – Les structures pyrénéennes du Languedoc et du golfe du Lion (Sud de la France). – *Bull. Soc. géol. Fr.*, **XXIII** (1), 51-63.
- AUDRA P., CAMUS H. & ROCHETTE P. (2001). – Le karst des plateaux jurassiques de la moyenne vallée de l’Ardèche: datation par paléomagnétisme des phases d’évolution plio-quaternaires (aven de la Combe Rajeau). – *Bull. Soc. géol. Fr.*, **172**, (1), 121-129.
- AUDRA P., MOCOCHAIN L., CAMUS H., GILLI E., CLAUZON G. & BIGOT J.-Y. (2004). – The effect of the Messinian deep-stage on karst development around the Mediterranean Sea. Examples from southern France. – *Geodin. Acta*, **17**, (6), 389-400.
- BACETA J.I., WRIGHT V.P., BEAVINGTON-PENNEY S.J. & PUJALTE V. (2007). – Palaeohydrogeological control of paleokarst macro-porosity genesis during a major sea-level lowstand: Danian of the Urbasa-Andia plateau, Navarra, North Spain. – *Sediment. Geol.*, **199**, 141-169.
- BACHE F., POPESCU S.-M., RABINEAU M., GORINI C., SUC J.-P., CLAUZON G., OLIVET J.-L., RUBINO J.-L., MELINTE-DOBRIANESCU M.-C., ESTRADA F., LONDEIX L., ARMIJO R., MEYER B., JOLIVET L., JOUANNIC G., LEROUX E., ASLANIAN D., TADEU DOS REIS A., MOCOCHAIN L., DUMURDŽANOV N., ZAGORCHEV I., LESIĆ V., TOMIĆ D., ÇAGATAY M.N., BRUN J.-P., SOKOUTIS D., CSATO I., UCARKUS G. & ÇAKIR Z. (2011). – A two step process for the re-flooding of the Mediterranean after the Messinian Salinity Crisis. – *Basin Res.*, **23**, 1-29.

- BARBARAND J., LUCAZEAU F., PAGEL M. & SÉRANNE M. (2001). – Burial and exhumation history of the southeastern Massif Central (France) constrained by an apatite fission-track thermochronology. – *Tectonophysics*, **335**, 275-290.
- BAUDRIMONT A. F. & DUBOIS P. (1977). – Un bassin mésogéen du domaine péri-Alpin: le sud-est de la France. – *Bull. Centres Rech. Explor.-Prod. Elf Aquitaine*, **1**, (1), 261-308.
- BENEDICTO A. (1996). – Modèles tectono-sédimentaires de bassins en extension et style structural de la marge passive du golfe du Lion (SE France). – Thèse Doctorat, Univ. Montpellier 2, 242p.
- BERNAOLA G., MARTIN-RUBIO M. & BACETA J.I. (2009). – New high resolution calcareous nannofossil analysis across the Danian/Selandian transition at the Zumaia section: comparison with south Tethys and Danish sections. – *Geol. Acta*, **7**, 79-92.
- BINNIE S.A., PHILLIPS W.M., SUMMERFIELD M.A., FIFIELD L.K. & SPOTILA J.A. (2008). – Patterns of denudation through time in the San Bernardino Mountains, California: Implications for early-stage orogenesis. – *Earth Planet. Sci. Lett.*, **276**, 62-72.
- BLAVOUX B., GILLI E. & ROUSSET C. (2004). – Alimentation et origine de la salinité de la source sous-marine de Port-Miou (Marseille-Cassis); principale émergence d'un réseau karstique hérité du Messinien. – *C. R. Acad. Sci., Paris, Géoscience*, **336** (6), 523-533.
- BONIOLY D., PERRIN J., ROURE F., BERGERAT F., COUREL L., ELMI S. & MIGNOT A. (1996). – The Ardèche paleomargin of the Southeast Basin of France: Mesozoic evolution of a part of the Tethyan continental margin. – *Mar. Petrol. Geol.*, **13** (6), 607-623.
- BRUXELLES L. (2001). – Dépôts et altérites des plateaux du Larzac central: Causses de l'Hospitalet et de Campestre (Aveyron, Gard, Hérault). Evolution morphogénétique, conséquences géologiques et implications pour l'aménagement. – Thèse Doctorat, Université d'Aix-Marseille I, 245p.
- BRUXELLES L., AMBERT P., GUENDON J.-L. & TRONCHETTI G. (1999). – Les affleurements de Crétacé supérieur sur les Grands Causses méridionaux (France). – *C. R. Acad. Sci., Paris*, **329**, 705-712.
- CALNER M., LEHNERT O. & NOLVAK J. (2010). – Palaeokarst evidence for widespread regression and subaerial exposure in the middle Katian (Upper Ordovician) of Baltoscandia: Significance for global climate. – *Palaeogeogr. Palaeoclimatol. Palaeoecol.*, **296**, 235-247.
- CAMUS H. (2001). – Evolution des réseaux hydrographiques au contact Cévennes-Grands Causses méridionaux: conséquences sur l'évaluation de la surrection tectonique. – *Bull. Soc. géol. Fr.*, **172** (5), 549-562.
- CAMUS H. (2003). – Vallée et réseaux karstiques de la bordure carbonatée sud-cévenole. Relation avec la surrection, le volcanisme et les paléoclimats. – Thèse Doctorat, Université Bordeaux III, 692p.
- CAMUS H., SERANNE M. & BASCHET J. (2004). – Karstic systems response to the Messinian-Pliocene extreme base-level changes on the onshore Gulf of Lion margin. Sea-level variations and aquifer management. – Abstract, H<sub>2</sub>O Symposium, Cannes.
- CANDE S. C. & KENT D. V. (1995). – Revised calibration of the geomagnetic polarity timescale for the Late Cretaceous and Cenozoic. – *J. Geophys. Res.*, **100**(B4), 6093-6095.
- CHAMPAGNAC J.-D., SCHLUNEGGER F., NORTON K., VON BLANCKENBURG F., ABBÜHL L.M. & SCHWAB M. (2009). – Erosion-driven uplift of the modern Central Alps. – *Tectonophysics*, **474**, (1-2), 236-249.
- CHARCOSSET P., COMBES P.-J., PEYBERNES B., CISZAK R. & LOPEZ M. (2000). – Pedogenic and karstic features at the boundaries of Bathonian depositional sequences in the Grands Causses area (southern France): stratigraphic implications. – *J. Sediment. Res.*, **70**, (1), 255-264.
- CLAUZON G. (1979). – Le canyon messinien de la Duranée (Provence, France): une preuve paléogéographique du bassin profond de dessiccation. – *Palaeogeogr. Palaeoclimatol. Palaeoecol.*, **29** (1-2), 15-40.
- CLAUZON G. (1982). – Le canyon messinien du Rhône: une preuve décisive du "dessicated deep-basin model (Hsü, Cita et Ryan, 1973). – *Bull. Soc. géol. Fr.*, **24**(3), 597-610.
- CLAUZON G., SUC J.-P., POPESCU S.M., MARUNTEANU M., RUBINO J.-L., MARINESCU F. & MELINTE M.C. (2005). – Influence of Mediterranean sea-level changes on the Dacic basin (eastern Paratethys) during the late Neogene: the Mediterranean Lago Mare facies deciphered. – *Basin Res.*, **17**(3), 437-462.
- COMBES P.-J. (1990). – Typologie, cadre géodynamique et genèse des bauxites françaises. – *Geodin. Acta*, **4** (2), 91-109.
- COMBES P.-J., PEYBERNES B. & FONDECAVE-WALLEZ M.-J. (2004). – Karsts polyphasés, faciès marins et continentaux dans le Paléocène de la partie orientale des Pyrénées françaises. – *Eclogae geol. Helv.*, **97**, 155-174.
- COMBES P.-J., PEYBERNES B., FONDECAVE-WALLEZ M.-J., SERANNE M., LESAGE J.-L. & CAMUS H. (2007). – Latest-Cretaceous/Paleocene karsts with marine infillings from Languedoc (south of France); paleogeographic, hydrogeologic and geodynamic implications. – *Geodin. Acta*, **20** (5), 301-326.
- COMBES P.-J., PEYBERNES B., FONDECAVE-WALLEZ M.-J., SERANNE M., LESAGE J.-L. & CAMUS H. (2008). – Reply to comment on Latest-Cretaceous/Paleocene karsts with marine infillings from Languedoc (south of France); paleogeographic, hydrogeologic and geodynamic implications. – *Geodin. Acta*, **21**, (3), 139-143.
- DEMANGEON P. (1959). – Contribution à l'étude de la sédimentation détritico dans le Bas-Languedoc. – Thèses d'Etat, Faculté des Sciences de Montpellier, 397p.
- FITZGERALD P., BALDWIN S.L., MUNOZ J.A., WEBB L. & SCHWABE E. (2005). – Exhumation of the Pyrenean intra-continental collisional orogen; new thermochronologic constraints from the central Pyrenees. – Geol. Soc. Amer., 2005 annual meeting, Salt Lake City, Utah, 346p.
- FREYTET P. (1970). – Les dépôts continentaux et marins du Crétacé supérieur et des couches de passage à l'Éocène en Languedoc. – Thèse Etat, Université de Paris, Orsay, 490p.
- FREYTET P. & PLAZIAT J.-C. (1982). – Continental carbonate sedimentation and pedogenesis – Late Cretaceous and early Tertiary of southern France. – *Contrib. Sediment.*, **12**, 1-213.
- GILLI E. & AUDRA P. (2004). – Les lithophages pliocènes de la fontaine de Vaucluse (Vaucluse, France) ; un argument pour une phase messinienne dans la genèse du plus grand karst noyé de France. – *C. R. Acad. Sci., Géoscience*, **336**, (16), 1481-1489.
- JAMES N.P. & CHOQUETTE P.W. (1988). – Paleokarst. – Springer-Verlag, New York, 416p.
- KOMINZ M.A., BROWING J.V., MILLER K.G., SUGARMAN P.J., MIZINTSEVA S. & SCOTSESE C.R. (2008). – Late Cretaceous to Miocene sea-level estimates from the New Jersey and Delaware coastal plain cores: an error analysis. – *Basin Res.*, **20**, 211-226.
- LACOMBE O. & JOLIVET L. (2005). – Structural and kinematic relationships between Corsica and the Pyrenees-Provence domain at the time of the Pyrenean Orogeny. – *Tectonics*, **24**(TC1003), 20p.
- LEGENDRE S., SIGE B., ASTRUC J.-G., BONIS L. DE, CROCHET J.-Y., DENYS C., GODINOT M., HARTEMBERGER J.-L., LEVEQUE F., MARANDAT B., MOURER-CHAUVIRE C., RAGE J.-C., REMY J.A., SUDRE J. & VIANEY-LIAUD M. (1997). – Les phosphorites du Quercy: 30 ans de recherche. Bilan et perspectives. – *Géobios, Mém. Spec.*, **20**, 331-345.
- LEMOINE M., BAS T., ARNAUD-VANNEAU A., ARNAUD H., DUMONT T., GIDON M., BOURBON M., GRACIANSKY P.C. DE, RUDKIEWICZ J.-L., MEGARD-GALLI J. & TRICART P. (1986). – The continental margin of the Mesozoic Tethys in the western Alps. – *Mar. Petrol. Geol.*, **3**, 179-199.
- LE STRAT P. (1975). – Le contexte géologique des minéralisations du Jurassique supérieur dans la basse vallée du Rieudort entre Sumène et Ganges. – Thèse doct. 3ème cycle, Univ. de Nantes, 167p.
- LOFI J., DEVERCHERE J., GAULLIER V., GORINI C., GUENOC P., LONCKE L., MAILLARD A., SAGE F. & THINON I. (2011). – Seismic atlas of the Messinian salinity crisis markers in the Mediterranean and Black seas. – Commission for the Geological map of the World / *Mém. Soc. géol. Fr.*, **179**, 72 p.
- LUCAS G., CROS P. & LANG J. (1976). – Etude microscopiques des roches meubles et consolidés. In: Les roches sédimentaires. – Doin Edit, Paris, 503p.
- MANGIN A. (1982). – Mise en évidence de l'originalité et de la diversité des aquifères karstiques. Originality and diversity of karstic aquifers. – *Ann. Scien. Univ. Besançon, Géologie*, **1**, 159-172.
- MARTINI E. (1971). – Standard Tertiary and Quaternary calcareous nannoplankton zonation. In: A. FARINACCI, Ed., Proceedings of the Second international Conference on Planktonic Microfossils, Roma. – Ed. Tecnoscienza, Rome, 2, 739-785.
- MELIM L.A. & SCHOLLE P.A. (2002). – Dolomitization of the Capitan Formation forereef facies (Permian, west Texas and New Mexico): seepage reflux revisited. – *Sedimentology*, **49**, (6), 1207-1227.

- MILLER K., KOMINZ M.A., BROWNING J.V., WRIGHT J.D., MOUNTAIN G.S., KATZ M.E., SUGARMAN P.J., CRAMER B.S., CHRISTIE-BLICK N. & PEKAR S.F. (2005). – The Phanerozoic record of global sea-level change. – *Science*, 310 p.
- MOCOCHAIN L., CLAUZON G. & BIGOT J.-Y. (2006). – Réponses de l'endokarst ardéchois aux variations eustatiques générées par la crise de salinité messinienne. – *Bull. Soc. géol. Fr.*, **177**, 27-36.
- MOLINA J.M., RUIZ-ORTIZA P.A. & VERAB J.A. (2000). – A review of polyphase karstification in extensional tectonic regimes: Jurassic and Cretaceous examples, Betic Cordillera, southern Spain. – *Sediment. Geol.*, **129**, (1-2), 71-84.
- NORTON K., VON BLANCKENBURG F., DIBIASE R., SCHLUNEGGER F. & KUBIK P. (2011). – Cosmogenic <sup>10</sup>Be-derived denudation rates of the eastern and southern European Alps. – *Internat. J. Earth Sci.*, **100**, (5), 1163-1179.
- PEDERSON J.L., ANDERS M.D., RITTENHOUR T.M., SHARP W.D., GOSSE J.C. & KARLSTROM K.E. (2006). – Using fill terraces to understand incision rates and evolution of the Colorado River in eastern Grand Canyon, Arizona. – *J. Geophys. Res. – Earth Surface*, **111**, (F2), 10.
- PEYBERNÈS B. & COMBES P.J. (1999). – Paléosurfaces d'érosion et paléokarsts dans la série de passage Crétacé / Tertiaire des Corbières occidentales (Aude, France). – *C. R. Acad. Sci., Paris*, **329**, 815-822.
- PEYBERNÈS B., FONDECAVE-WALLEZ M.-J. & COMBES P.-J. (2001). – Mise en évidence d'un sillon marin à brèches dano-sélandiennes dans les Pyrénées centrales (Zone Interne Métamorphique et Zone Nord-Pyrénéenne). – *C. R. Acad. Sci., Paris*, **332**, 379-386.
- PEYBERNÈS B., CISZACK R., FONDECAVE-WALLEZ M.-J., COMBES P.-J., CAMUS H. & SÉRANNE M. (2003). – Présence de Paléocène marin dans les Grands Causses (France). – *C. R. Geoscience*, **335**, 681-689.
- PHILIP H., MATTAUER M., BODEUR Y., SEGURET M., PUECH J.-P. & MATTEI J. (1978). – Carte géologique de la France au 1/50 000. Feuille de St Martin de Londres. – BRGM, Orléans.
- PLAGNES V., CAUSSE C., GENTY D., PATERNE M. & BLAMART D. (2002). – A discontinuous climatic record from 187 to 74 ka from a speleothem of the Clamouse Cave (south of France). – *Earth Planet. Sci. Lett.*, **201**, (1), 87-103.
- QING H., BOSENCE D.W.J. & ROSE E.P.F. (2001). – Dolomitization by penesaline sea water in Early Jurassic peritidal platform carbonates, Gibraltar, western Mediterranean. – *Sedimentology*, **48**, (1), 153-163.
- ROTH P.H. & KRUMBACH K.R. (1986). – Middle Cretaceous calcareous nanofossil biogeography and preservation in the Atlantic and Indian oceans; implications for paleoceanography. – *Mar. Micropal.*, **10**, 235– 266.
- SÉRANNE M. (1999). – The Gulf of Lion continental margin (NW Mediterranean) revisited by IBS: an overview. In: B. DURAND, L. JOLIVET, F. HORVÁTH and M. SÉRANNE, Eds, The Mediterranean basins: Tertiary extension within the Alpine orogen. – *The Geol. Soc. Sp. Publ.*, **156**, London, 15-36.
- SÉRANNE M., BENEDICTO A., TRUFFERT C., PASCAL G. & LABAUME P. (1995). – Structural style and evolution of the Gulf of Lion Oligo-Miocene rifting: Role of the Pyrenean orogeny. – *Mar. Petrol. Geol.*, **12**, 809-820.
- SÉRANNE M., CAMUS H., LUCAZEAU F., BARBARAND J. & QUINIF Y. (2002). – Surrection et érosion polyphasées de la bordure cévenole – Un exemple de morphogenèse lente. – *Bull. Soc. géol. Fr.*, **173**, (2), 97-112.
- TREMOLADA F., SCIUNNACH D., SCARDIA G. & PREMOLI-SILVA I. (2008). – Maastrichtian to Eocene calcareous nanofossil biostratigraphy from the Tabiago section, Brianza area, northern Italy. – *Riv. It. Pal. Strat.*, **114**, 29-39.
- VAN HENGSTUM P.J., SCOTT D.B. & JAVAUX E.J. (2009). – Foraminifera in elevated Bermudian caves provide further evidence for +21 m eustatic sea level during marine isotope stage 11. – *Quatern. Sci. Rev.*, **28** (19-20), 1850-1860.
- WADE B.S., PEARSON P.N., BERGGREN W.A. & PÄLIKE H. (2011). – Review and revision of Cenozoic tropical planktonic foraminiferal biostratigraphy and calibration to the geomagnetic polarity and astronomical time scale. – *Earth-Science Rev.*, **104**, 111-142.
- WRIGHT D.T. & WACEY D. (2005). – Precipitation of dolomite using sulphate-reducing bacteria from the Coorong Region, south Australia: significance and implications. – *Sedimentology*, **52**, (5), 987-1008.